Department Of Energy Quarterly Technical Report

4/15/95

Roger N. Anderson

Lamont-Doherty
Earth Observatory

Reporting Period: 1/95-3/95
DE-FC22-93BC14961
Award Date: July 15, 1993
Completion Date: 10/30/95
Government Award for Phase 2: $2,052,801
COR: James P. Lewis
Columbia University

DISCLAIMER

Lamont-Doherty Earth Observatory

GBRN/DOE Project
"Dynamic Enhanced Recovery Technologies"

DOE Contract #:DE-FC22-93BC14961

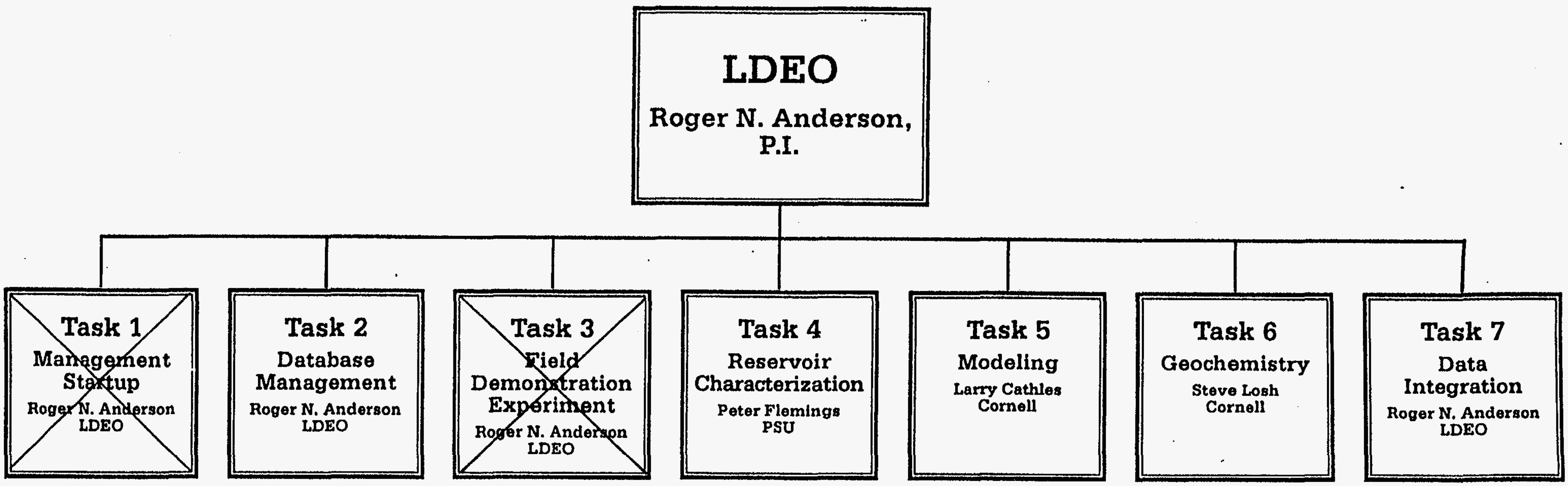

* designates primary file location

Dynamic Enhanced Recovery Technologies

Task No.	Name	Scheduled Start	Scheduled Finish
1	Management Startup	8/1/92	6/16/94
1.1	Personnel and computer acquisitions	8/1/92	12/31/93
1.1.1	Staffing up and set up of office	8/1/92	12/31/93
1.1.2	Computer purchases	8/1/92	12/31/93
1.1.3	Signed DOE contract	7/15/93	7/15/93
1.2	Insurance negotiations	8/1/92	12/31/93
1.3	Technology transfer	1/15/93	6/16/94
1.3.1	GBRN semi-annual meeting, Houston	1/15/93	1/15/93
1.3.2	AAPG exhibition booth @ convention	4/23/93	4/28/93
1.3.3	GBRN semi-annual meeting, Baton Rouge	6/7/93	6/9/93
1.3.4	GBRN Semi-Annual Meeting, Houston	1/31/94	2/1/94
1.3.5	AAPG Exhibition Booth @ convention	6/13/94	6/15/94
1.3.6	AAPG Poster Session	6/13/94	6/13/94
1.3.7	GBRN Semi-Annual Meeting, Denver	6/16/94	6/16/94
2	Database Management	8/1/92	10/31/95
2.1	Fluid flow monitoring of multiple 3-D seismic datasets	8/1/92	6/30/95
2.2	Geological analysis of Pennzoil & Tex/Chev 3-D datasets	10/1/92	10/31/95
2.3	Real Time visulation of Database	10/1/92	9/30/95
2.4	3-D interpretation of Shell/Exxon 3-d seismic datset	6/1/94	10/31/95
2.5	Reformat Data for Res Simluation	7/1/94	10/31/95
3	Field Demonstration Experiment	8/1/92	4/30/95
3.1	Environmental Assessment	8/1/92	12/31/93
3.2	Field demonstration supervision	5/1/93	12/25/93
3.2.1	Pre-spud meeting with Pennzoil and vendors	5/1/93	10/22/93
3.2.2	Spud Pathfinder well	11/2/93	11/2/93
3.2.3	GBRN well extension begins	11/23/93	11/23/93
3.2.4	Pathfinder well completed	12/25/93	12/25/93
3.3	Interpretation of results of well experiments	4/1/93	4/30/95
3.3.1	Arrange contractual relationships with appropriate parties	4/30/93	2/28/94
3.3.2	Acquisition of borehole data	11/23/93	12/25/93
3.3.3	Interpretation of borehole data	11/2/93	3/31/95
3.3.4	Petroleum engineering	4/1/93	4/30/95
3.3.5	Production facilities management	8/1/93	12/31/93
3.3.6	Production of fault zone distributary management	11/1/93	12/25/93
4	Reservoir Characterization	10/1/92	10/31/95
4.1	Stratigraphic interpretation	10/1/92	5/31/95
4.1.1	16 Block 2-D Analysis	10/1/92	4/1/94
4.1.2	4 Block 3-D Analysis	10/1/92	5/31/95
4.1.3	North-South Transects	10/1/92	5/1/94
4.2	Salt analysis and paleogeographic reconstruction	10/1/92	8/1/95
4.2.1	North-South Transects	10/1/92	3/1/94
4.2.2	16 Block 3-D Restoration	10/1/92	8/1/95
4.3	Fluid potential analysis	10/1/92	10/31/95
4.3.1	Fault plane mapping	10/1/92	10/31/95
4.3.2	Structure maps	10/1/92	7/31/94
4.3.3	3-D permeability pathway	6/1/94	10/31/95

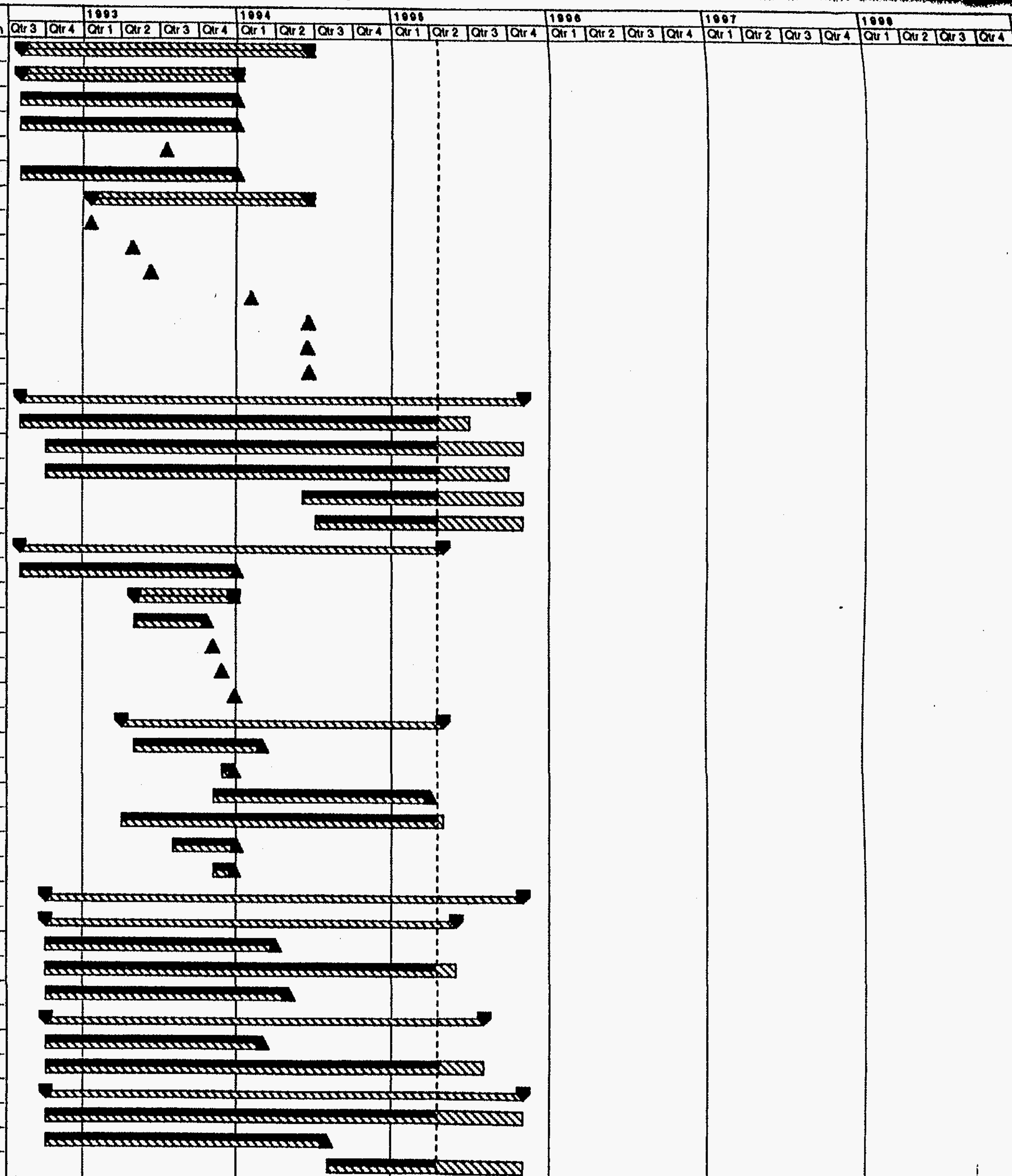

PON: DE-PS22-93BC14961
10/15/94

Critical · Noncritical · Milestone at completion · Milestone · Completed Milestone · Summary · Progress

Dynamic Enhanced Recovery Technologies

Task No.	Name	Scheduled Start	Scheduled Finish
4.3.4	Pressure mapping	10/1/92	10/31/95
4.3.5	Temperature mapping	10/1/92	10/31/95
4.4	Amplitude mapping analysis	10/1/92	10/31/95
5	Modeling	10/1/92	10/31/95
5.1	Geologic input	10/1/92	10/31/95
5.1.1	2-D flat files	10/1/92	6/30/93
5.1.2	3-D flat files	3/1/93	4/30/94
5.1.3	Realistic 3-D SEI description	6/1/93	2/28/95
5.1.4	Present porosity distribution	10/1/92	2/28/95
5.1.5	RVE 2-D seismic lines	10/1/92	2/28/95
5.1.6	Near-fault details	10/1/93	10/31/95
5.1.7	History of salt movement	1/1/93	6/30/95
5.1.8	Continuing modification of geologic input	7/1/94	6/30/95
5.1.9	Geologic and geochemical observations	4/1/95	10/31/95
5.2	Model simulations	10/1/92	10/31/95
5.2.1	2-D cross sections	10/1/92	6/30/93
5.2.2	3-D demonstrations	2/1/93	6/30/95
5.2.3	3-D realistic SEI simulation	8/1/93	8/31/95
5.2.4	Specific modeling investigations	1/1/94	10/30/95
5.2.5	Model synthesis	6/1/95	10/31/95
5.2.6	Final modeling investigations	6/1/95	10/31/95
5.3	Akcess.basin preparation	10/1/92	10/30/95
5.3.1	3-D template	10/1/92	12/31/94
5.3.2	Adaptation of Akcess.basin for parallel execution	3/1/93	2/28/95
5.3.3	Two-phase templates	7/1/93	10/30/95
5.3.4	Consultation and continued tuning of Ackess.basin	2/28/94	6/30/95
5.4	Fortran algorithms	10/1/92	3/31/95
5.4.1	Diapirism and Compaction	10/1/92	12/31/94
5.4.2	Fault Movement	2/1/93	12/31/94
5.4.3	Physical Property Algorithms	10/1/93	3/31/95
5.4.4	Inorganic Alteration Algorithms	4/1/94	1/31/95
5.5	Chemical models	10/1/92	6/30/95
5.5.1	Gas solubility and gas generation kinetics	10/1/92	4/30/95
5.5.2	Inorganic 1-D alteration models with gas phase present	6/30/93	4/30/95
5.5.3	Equilibrium inorganic chemical alteration	10/1/92	6/30/95
5.5.4	Isotopic alteration	7/1/94	6/30/95
5.6	Visualization of model output	1/1/93	10/31/95
5.6.1	Installation of common computing environment-all GBRN sit	1/1/93	9/30/93
5.6.2	Standardized input data file and 2-D macrofile generation	1/1/93	10/31/95
5.6.3	Visualization and image transmission	1/1/93	10/31/95
6	Geochemistry	9/1/92	12/31/95
6.1	Inorganic geochemistry	9/1/92	10/31/95
6.1.1	Petrographic analysis	10/1/92	6/30/95
6.1.1.a	Complete 75 samples	10/1/92	3/31/94
6.1.1.b	Complete 175 samples	4/1/94	6/30/95
6.1.2	Cathodoluminescence	9/1/93	6/30/95

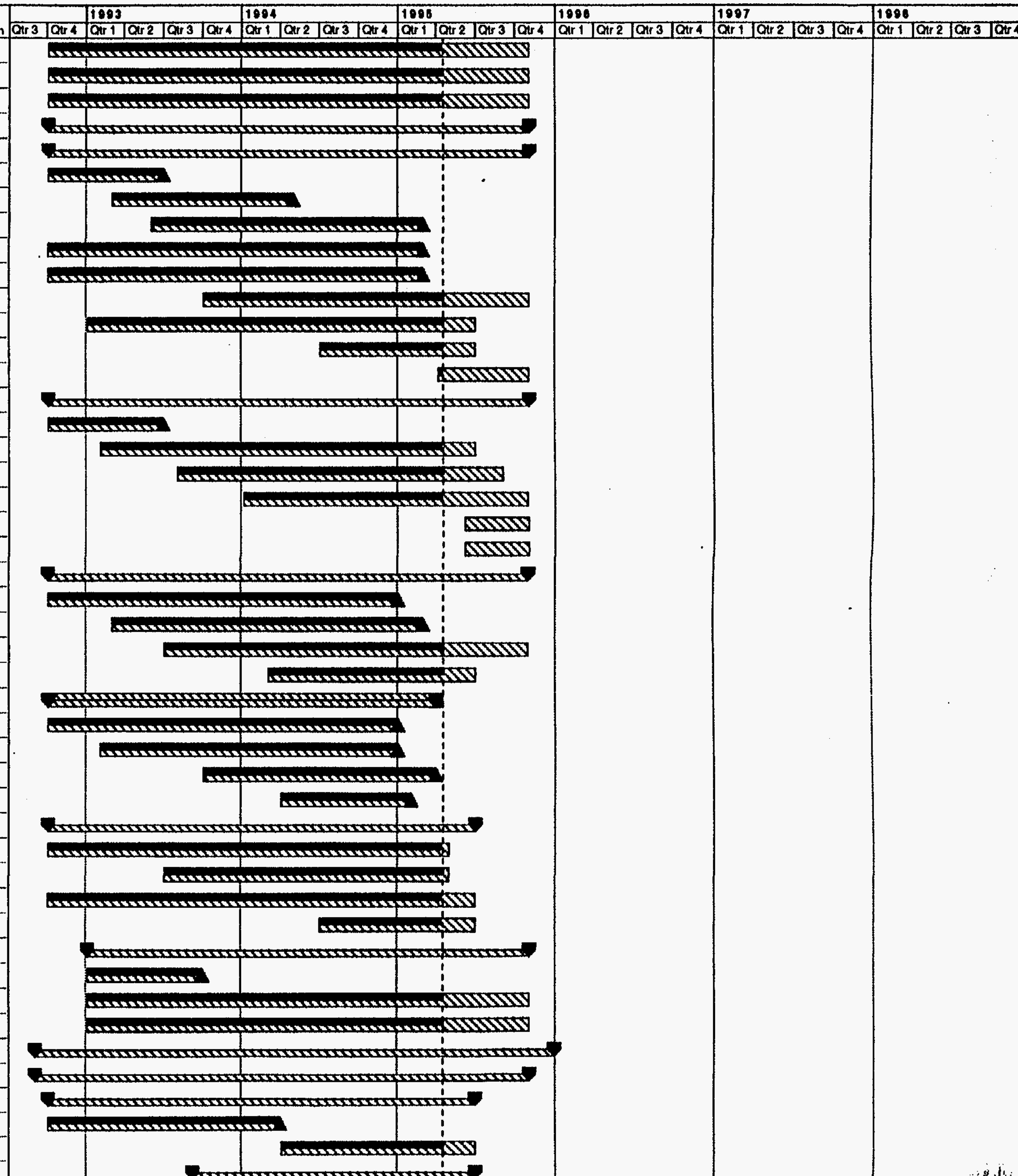

Dynamic Enhanced Recovery Technologies
1993 1994 1995 1996 1997 1998

6.1.2 Cathodoluminescence 9/1/93 6/30/95

PON: DE-PS22-93BC14961 Critical Milestone at completion Completed Milestone Progress

Dynamic Enhanced Recovery Technologies

Task No.	Name	Scheduled Start	Scheduled Finish
6.1.2.a	Complete 25 samples	9/1/93	6/30/95
6.1.2.b	Complete 75 samples	4/1/94	6/30/95
6.1.3	Fluid Inclusions Omitted - Lack of Data	4/20/94	4/20/94
6.1.4	X-ray diffraction	3/1/93	10/31/95
6.1.4.a	Complete 25 hours	3/1/93	6/30/94
6.1.4.b	Complete 50 hours	7/1/94	6/30/95
6.1.4.c	Complete 25 hours	7/1/95	10/31/95
6.1.5	Smectite-illite transformation	9/1/93	10/31/95
6.1.5.a	Complete 50 hours	9/1/93	12/31/93
6.1.5.b	Complete 125 hours	1/1/94	12/31/94
6.1.5.c	Complete 50 hours	1/1/95	6/30/95
6.1.5.d	Complete 25 hours	7/1/95	10/31/95
6.1.6	Electron microprobe analysis	9/1/92	6/30/95
6.1.6.a	Complete 25 hours	9/1/92	6/30/94
6.1.6.b	Complete 100 hours	7/1/94	3/31/95
6.1.6.c	Complete 25 hours	4/1/95	6/30/95
6.1.7	Scanning electron microscopy	3/1/93	6/30/95
6.1.7.a	Complete 25 hours	3/1/93	6/30/94
6.1.7.b	Complete 100 hours	7/1/94	3/31/95
6.1.7.c	Complete 25 hours	4/1/95	6/30/95
6.1.8	Bulk chemical analysis	1/1/94	10/31/95
6.1.8.a	Complete 50 samples	1/1/94	6/30/94
6.1.8.b	Complete 50 samples	7/1/94	6/30/95
6.1.8.c	Complete 20 samples	7/1/95	10/31/95
6.1.9	Carbonate C and O isotopes	4/1/94	10/31/95
6.1.9.a	Complete 100 samples	4/1/94	12/31/94
6.1.9.b	Complete 100 samples	1/1/95	6/30/95
6.1.9.c	Complete 50 samples	7/1/95	10/31/95
6.1.10	Strontium isotopic fluid analysis	7/1/94	12/31/94
6.1.10.a	Complete 10 samples	7/1/94	12/31/94
6.1.11	Fluid analysis	9/1/93	12/31/94
6.1.11.a	Complete 20 samples	9/1/93	12/31/93
6.1.11.b	Complete 10 samples	10/31/94	12/31/94
6.2	Organic geochemistry	9/1/93	12/31/95
6.2.1	Hydrous pyrolsis	9/1/93	7/30/95
6.2.1.a	Complete 2 experiments	9/1/93	12/31/93
6.2.1.b	Complete 2 experiments	1/1/94	6/30/94
6.2.1.c	Complete 2 experiments	7/1/94	12/31/94
6.2.1.d	Complete 2 experiments	1/1/95	7/30/95
6.2.2	Organic chemistry, petrography, isotopes	12/1/93	6/30/95
6.2.2.a	Complete 30 samples	12/1/93	6/30/94
6.2.2.b	Complete 400 samples	7/1/94	6/30/95
6.2.3	Modeling and technology transfer	10/1/93	12/31/95
6.2.3.a	Complete paper on GBRN data	10/1/93	10/1/93
6.2.3.b	Complete hydrous pyrolsis paper	12/31/95	12/31/95
7	Integration of Drilling, Data & Modeling Results	3/1/94	1/15/96

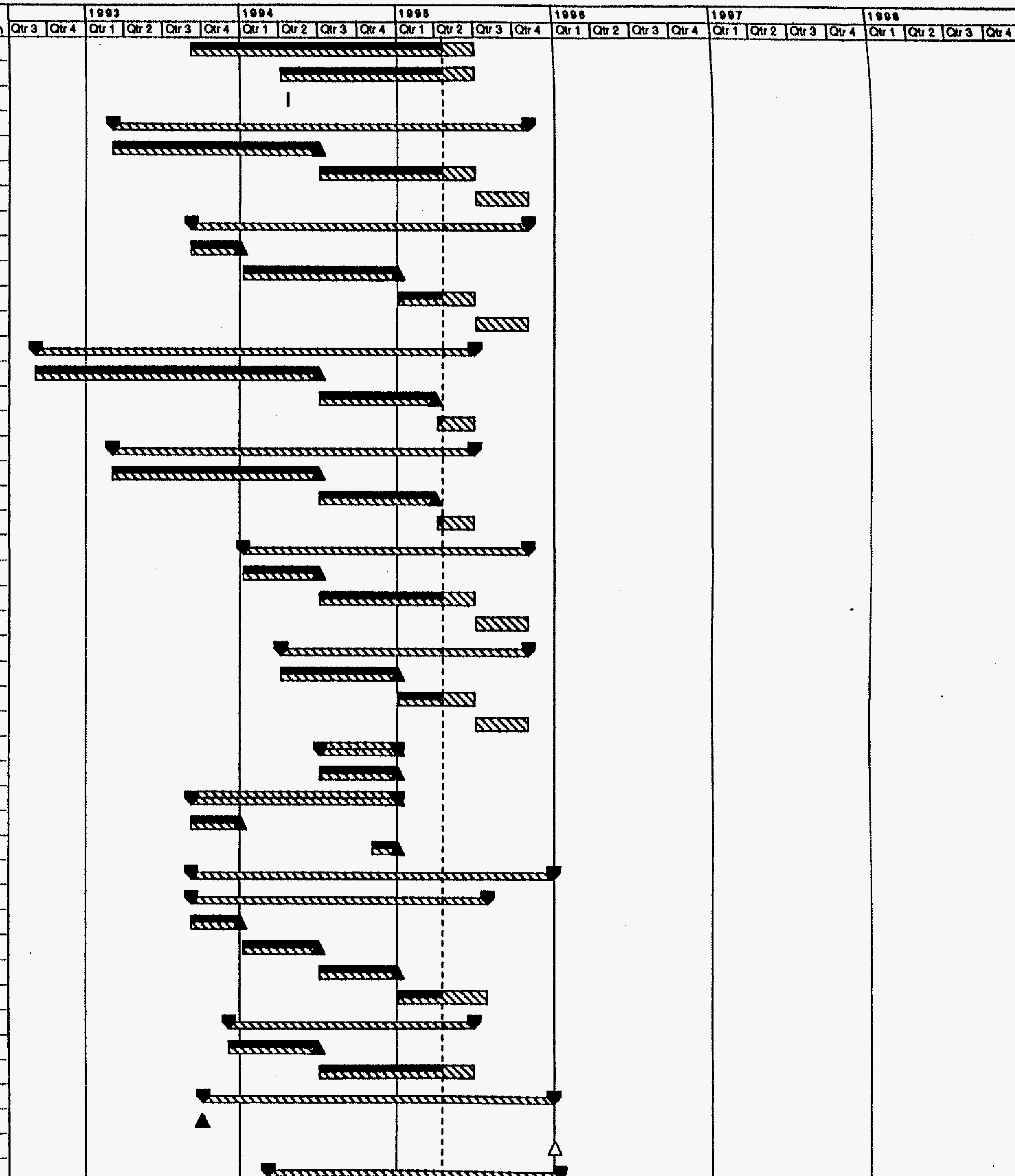

PON: DE-PS22-93BC14961
10/18/94

Critical — Milestone at completion — Completed Milestone — Progress

Noncritical — Milestone — Summary

Dynamic Enhanced Recovery Technologies

Task No.	Name	Scheduled Start	Scheduled Finish
7.1	Interaction of fluid flow simulation & database	7/1/94	10/31/95
7.2	Publication of results	3/1/94	10/31/95
7.2.1	Well Data Volume-CD-ROM	3/1/94	3/5/95
7.2.2	Publications & Abstracts	7/1/94	10/31/95
7.3	US reserves re-evaluation	6/1/94	9/30/95
7.4	Technology transfer	10/23/94	1/15/96
7.4.1	SEG convention	10/23/94	10/27/94
7.4.2	GBRN semi-annual meeting	3/2/95	3/2/95
7.4.3	AAPG convention	3/5/95	3/8/95
7.4.4	GBRN semi-annual meeting	7/15/95	7/15/95
7.4.5	SEG convention	11/5/95	11/9/95
7.4.6	GBRN semi-annual meeting	1/15/96	1/15/96

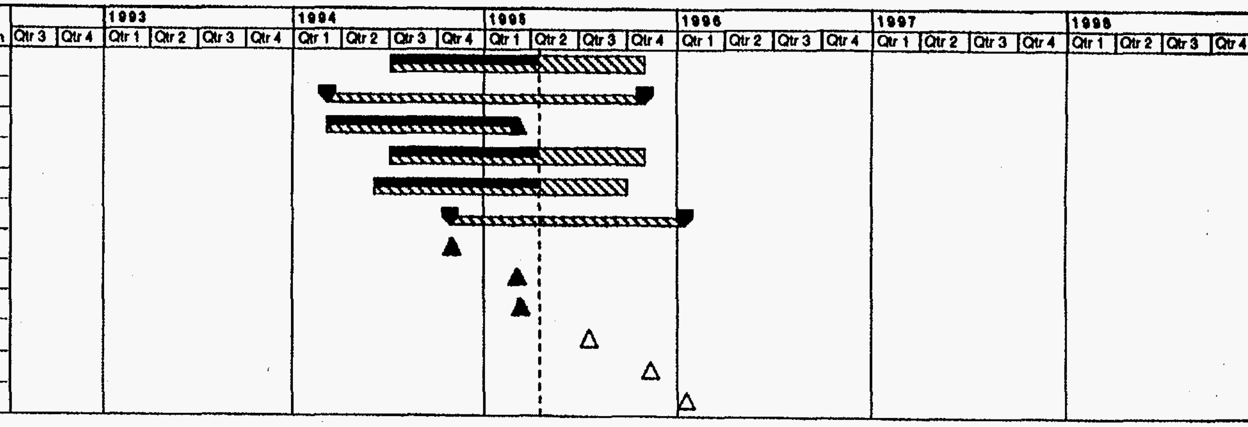

PON: DE-PS22-93BC14961 | Critical | Milestone at completion | Completed Milestone | Progress

TASK ONE

MANAGEMENT

START-UP

Roger N.Anderson
LDEO

PON: DE-PS22-93BC14961 Critical Milestone at completion Completed Milestone Progress

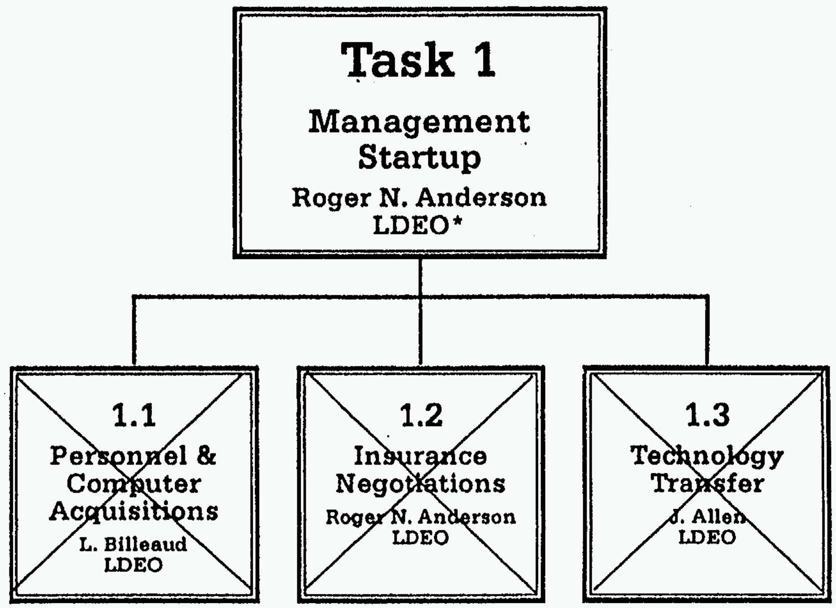
Task 1
Management Startup
Roger N. Anderson
LDEO*
1.1
Personnel & Computer Acquisitions
L. Billeaud
LDEO
1.2
Insurance Negotiations
Roger N. Anderson
LDEO
1.3
Technology Transfer
J. Allen
LDEO

Task One - Management Start-Up
Roger N. Anderson - Task Manager

OBJECTIVES: The purpose of this task to was equip the project with staff and resources (computer and otherwise) to accomplish the other 6 tasks of this project; to negotiate contracts with several industry and university subcontractors to achieve the task objectives; and to initiate the technology transfer to industry and the public from the very beginning of this project.

SUMMARY OF TECHNICAL PROGRESS:

This task was completed in Phase I of our project. Technology Transfer will be discussed in Task 7 during Phase II.

TASK TWO

DATABASE

MANAGEMENT

Roger N.Anderson
LDEO

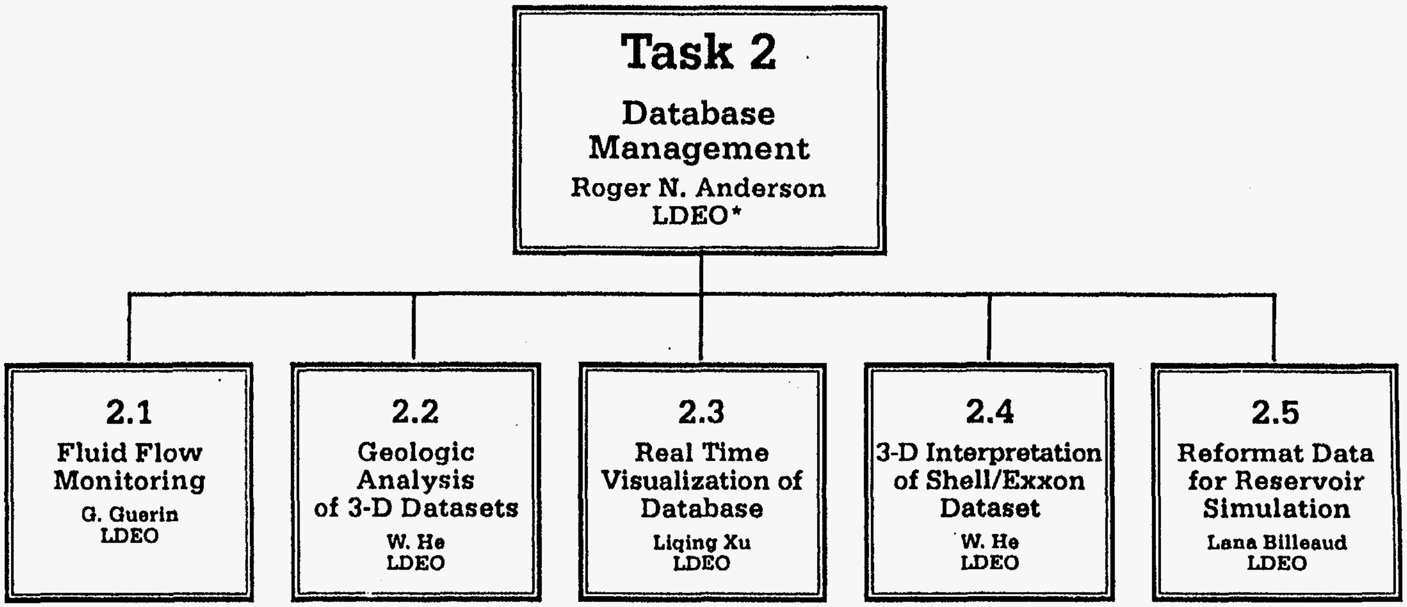
Task 2
Database Management
Roger N. Anderson
LDEO*
2.1
Fluid Flow Monitoring
G. Guerin
LDEO
2.2
Geologic Analysis of 3-D Datasets
W. He
LDEO
2.3
Real Time Visualization of Database
Liqing Xu
LDEO
2.4
3-D Interpretation of Shell/Exxon Dataset
W. He
LDEO
2.5
Reformat Data for Reservoir Simulation
Lana Billeaud
LDEO

Task Two - Database Management
Roger N. Anderson - Task Manager

OBJECTIVES: The objectives of this task are to accumulate, archive, and disseminate the geological information available within the area of research of this project; networked database creation, generation of new seismic interpretation with high-tech software, and real-time visualization of the on-line database.

SUMMARY OF TECHNICAL PROGRESS:

2.1 Fluid-Flow Monitoring Using Industry Multiple 3-D Seismic Data Sets: We are currently integrating the 1992 Shell/Exxon data set (received December 1994) with the two 3-D seismic surveys, the Texaco/Chevron data set and the Pennzoil et al data set.

Liqing Xu added three additional AVS modules to the 4-D package library and modified, debugged previously coded AVS modules. Liqing also worked on 4-D images and completed a new 4-D computer demonstration for the APPG convention held in Houston, Texas in late March 1995.

2.2 Geological Analyses of Industry 3-D Seismic Surveys: Landmark has completed its task of comparing the traditional interpretation of the horizons and faults and the reinterpreted reflector horizons and faults in Phase I of this project. The reinterpreted geologic data was converted and exported to other databases as per previous reports. Integration of several data sets aided in the reassessment of the drilling location and the field demonstration experiment.

Lincoln Pratson is continuing phase three of the development of an algorithm for well log/time series correlation and is nearing completion. In phases one and two, the shape-amplitude matching component and book-keeping component of the algorithm were implemented. Phase three has focused on implementing a statistical scheme for ranking all possible correlations between any two related time series, specifically the well logs in Eugene Island 330. Initial efforts have focused on using statistical measures, such as the chi-square test of similarity, which assume time series differences have a Gaussian distribution. Ongoing analyses of well-log simulation results indicate this assumption may not be valid. To make the algorithm more robust, non-parametric correlation statistics (i.e., measures that do not require Gaussian sample distributions) are now being explored for use in the algorithm instead.

2.3 Real-Time Visualization of Database: Our real-time database is on-line. Currently, L-DEO, LSU, PSU, and Cornell have the capability of sharing data and results. Our World Wide Web is online now. Anyone on the Internet can browse through our database, provided that they have a HTML document browser installed. The link is named: http://www.ldeo.columbia.edu/GBRN/GBRN_Brochure. We are still working on adding the DOE reports to the database.

2.4 3-D Interpretation of the Shell/Exxon 3-D Seismic Data: We received the Shell 3-D seismic survey in December 1994. We are currently merging it into our 4-D AVS analyzed system so that we can difference that data set with the Pennzoil and Texaco/Chevron 3-D surveys. The 4-D analyses will be limited using this 3-D dataset.

2.5 Reformat Data Volumes for Simulation: The reservoir simulation goal has been changed to investigating the LF sand data.

TASK THREE

FIELD

DEMONSTRATION

EXPERIMENT

Roger N. Anderson
LDEO

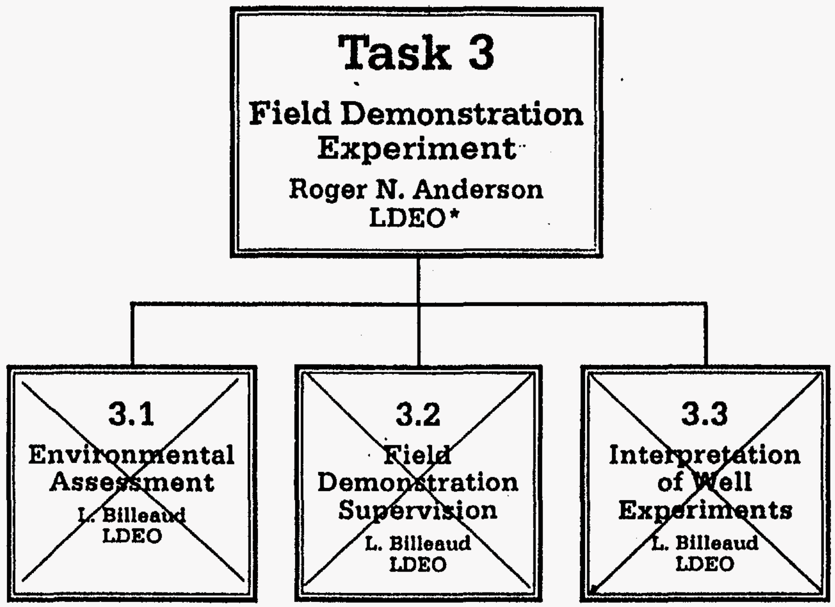
Task 3
Field Demonstration Experiment
Roger N. Anderson
LDEO*
3.1
Environmental Assessment
L. Billeaud
LDEO
3.2
Field Demonstration Supervision
L. Billeaud
LDEO
3.3
Interpretation of Well Experiments
L. Billeaud
LDEO

TASK FOUR

RESERVOIR

CHARACTERIZATION

Peter Flemings - Penn State

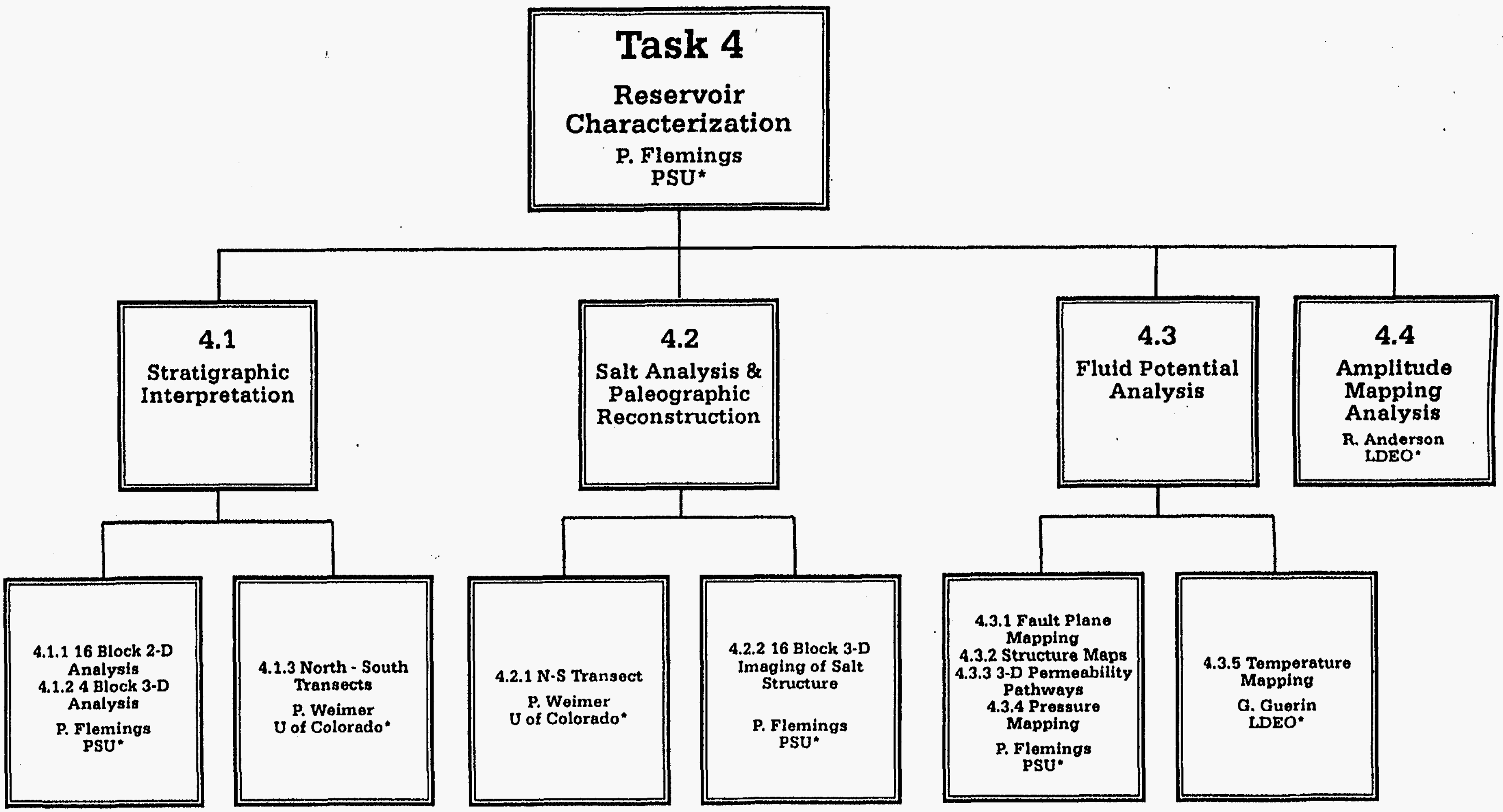
Task 4
Reservoir Characterization
P. Flemings
PSU*
4.1
Stratigraphic Interpretation
4.2
Salt Analysis & Paleographic Reconstruction
4.3
Fluid Potential Analysis
4.4
Amplitude Mapping Analysis
R. Anderson
LDEO*
4.1.1 16 Block 2-D Analysis
4.1.2 4 Block 3-D Analysis
P. Flemings
PSU*
4.1.3 North - South Transects
P. Weimer
U of Colorado*
4.2.1 N-S Transect
P. Weimer
U of Colorado*
4.2.2 16 Block 3-D Imaging of Salt Structure
P. Flemings
PSU*
4.3.1 Fault Plane Mapping
4.3.2 Structure Maps
4.3.3 3-D Permeability Pathways
4.3.4 Pressure Mapping
P. Flemings
PSU*
4.3.5 Temperature Mapping
G. Guerin
LDEO*

Task 4 - Reservoir Characterization
Peter Fleming - Task Manager

1.0 Overview

An outline of the individual tasks is provided below. Primary responsibility for tasks is shown in parentheses: PSU = Penn State University, CU = University of Colorado- Boulder, LDEO = Lamont-Doherty Earth Observatory. Completed tasks are indicated by a pound sign (#). A change in completion date of the subtask is indicated by an asterisk (*).

Task #	Name	Start	Finish
Task 4:	Reservoir Characterization	10/92	10/95
4.1:	Stratigraphic Interpretation		
4.1.1:	16 Block 2-D Analysis (PSU)	10/92	4/94 #
4.1.2:	4 Block 3-D Analysis (PSU)	10/92	5/95 *
4.1.3:	North-South Transects (CU)	10/92	5/94 #
4.2:	Salt Analysis and Paleogeographic Reconstruction		
4.2.1:	North-South Transects (CU & PSU)	10/92	3/94 #
4.2.2:	16 Block 3-D Restoration (CU)	10/92	8/95
4.3:	Fluid Potential Analysis		
4.3.1:	Fault Plane Mapping (PSU)	10/92	10/95*
4.3.2:	Structure Maps (PSU)	10/92	7/95 *
4.3.3:	3-D Permeability Pathways (PSU)	8/94	10/95
4.3.4:	Pressure Mapping (PSU)	10/92	6/94 #
4.3.5:	Temperature Mapping (G. Guerin, LDEO)		
4.4:	Amplitude Mapping Analysis (R. Anderson, LDEO)		

2.0 Acquisition of A-12 Core

PSU has received core photographs, the Sedimentology and Petrology Report, and all paper logs run on the A-12 well, including FMI, Dipmeter, and Thin Bed Analysis. The whole core is currently being held at Core Laboratories, Houston, for further analysis. The PSU Core Repository will receive the core as soon as it is released.

3.0 Progress Made by Subtask

4.1: Stratigraphic Interpretation
Original: 10/92-11/94 Current: 10/92-1/95

4.1.1: 16 Block 2-D analysis (PSU)
Original Projection: 10/93
Current Projection: 4/94

This subtask has been completed. Details of this work have been accepted for publication by the AAPG Bulletin. The paper is by Alexander and Flemings and is entitled, "Stratigraphic Architecture and Evolution of a Plio-Pleistocene Salt Withdrawal Mini-Basin: Eugene Island, South Addition, Block 330, Offshore Louisiana." This paper was released in the PSU Annual Report, July, 1994.

4.1.2: 4 Block 3-D analysis (PSU)
Original Projection: 11/94
Current Projection: 5/95

On March 2, 1995 Bruce Hart presented a paper (on behalf of himself and co-authors David Sibley and Peter Flemings) and poster at the GBRN corporate affiliates meeting in Houston that summarizes the results of their work on the depositional controls on reservoir character of the GA Sand. The following day, Hart was invited to present a talk on the architecture and reservoir characteristics of lowstand/shelf margin deltas to a joint meeting of the Sequence Stratigraphy and Structural Geology Resources Team and Advanced Exploration Organization of Conoco Inc. in Houston. Following these presentations and discussions held with other scientists at the AAPG Meeting in Houston, several new concepts were developed that are now being incorporated into the manuscript on the GA Sand by Hart, Sibley and Flemings (e.g., Figure 1).

Work continues on mapping other horizons in the 3-D seismic data. Of particular note is mapping (using the Pennzoil, Texaco and Shell seismic volumes) and reservoir characterization of the LF sand in the "A" fault block (four corners area of Blocks 330, 331, 337 and 338). This is a blocky sand, considerably different from the GA sand in its internal facies architecture and production characteristics. By integrating production data with the geologic mapping, we are able to make simple models that describe the drainage of the sand and accompanying fluid contact levels (oil/water, gas/oil; Figure 2). The high amplitude patterns visible on maps of this sand suggest a much more uniform fluid distribution than in the GA (i.e., less compartmentalization), although some details of the production data suggest that the LF is a more complicated reservoir than might be expected. Aspects of this work were incorporated in a talk presented by Roger Anderson at the GBRN Corporate Affiliates meeting on March 2.

4.1.3: North-South Transects (CU)
Original Projection: 10/93
Current Projection: 5/94

This subtask is complete. See Task 4.2.1 for reporting.

4.2: Salt Analysis and Paleogeographic Reconstruction
Original: 10/92-11/94 Current: 10/92-8/95

4.2.1: North-South Transects (CU & PSU)
Original Projection: 10/94
Current Projection: 3/94

This subtask is complete. Details of this work, and the results from Subtask 4.1.3, will be presented in three parts:

1) Rowan, M. G., Weimer, P., Flemings, P.B., "Three-dimensional geometry and evolution of a composite, multi-level salt system, western Eugene Island, offshore Louisiana," submitted to Gulf Coast Geological Societies, v. 43.

2) Rowan, M. G., Weimer, P., Flemings, P.B., "Deformation of a composite salt system: controls on the structural and stratigraphic evolution of the Eugene Island Block 330 minibasin, Gulf of Mexico," to be submitted to AAPG Bulletin.

3) Rowan, M. G., Weimer, P., Budhijanto, F., Flemings, P.B., "Integrated Regional Stratigraphic Sequence and Structural Framework and Geological Evolution of the Eugene Island Block 330 Area, Offshore Louisiana," submitted to DOE.

4.2.2: 16 Block 3-D Restoration (CU)
Original Projection: 11/94
Current Projection: 8/95

This subtask awaits the completion of horizon and fault plane structure maps (subtask 4.3.2).

4.3: Fluid Potential Analysis (PSU)
Original: 10/92-10/95 Current: 10/92-10/95

4.3.1: Fault Plane Mapping (PSU)
Original Projection: 9/94
Current Projection: 10/95

Fault plane mapping awaits completion of the structure mapping subtask (4.3.2 below). Hart and Bishop are currently interpreting horizons and fault planes in Landmark's SeisWorks. Mark Rowan will visit Penn State this quarter to ensure that the maps are in appropriate format for fault plane interpretation. Rowan will work on the fault plane mapping and Hart and Rowan will develop a fill and spill algorithm to study the evolution of secondary migration in this area.

4.3.2: Structure Maps (PSU)
Original Projection: 9/94
Current Projection: 7/95

Work continues on this subtask at a steady pace. We have finished mapping the GA sand and are actively interpreting the HB sand. We will soon finish mapping the JD, KE, LF, MG, OI, and Lentic surfaces.

4.3.3: 3-D Permeability Pathways (PSU)
Original Projection: 10/95
Current Projection: 10/95

The last quarter has focused on the detailed interpretation of the stress field as inferred from stress measurements made in the Pathfinder Well. The basic interpretation of the stress measurements is now complete and is in the Pathfinder CD-ROM in a paper entitled "State of Stress in the Pathfinder Well."

4.3.4: Pressure Mapping (PSU)
Original Projection: 7/93
Current Projection: 6/94

Work on this subtask is complete. Details of this work can be found in:

Hart, B.S., Flemings, P.B., and Deshpande, A. Porosity and pressure: Role of compaction disequilibrium in the development of geopressures in a Gulf Coast Pleistocene basin. Geology 23(1): 45-48 (1995).

Task 4.3.4 - Pressure Mapping

Pavel Peska interpreted the caliper logs to constrain in situ stress in the South Eugene Island field. Analysis of borehole breakouts detected in deviated wells by caliper logs was extended from the Pathfinder well to other wells in the South Eugene Island field where the logs were available (wells A2, A6, A20, A21, A22, #11 in the block 330, wells A11 and A12 in the block 316 and well A8 in the block 338). Borehole enlargements at azimuths which do not correlate with the hole inclination were detected in the wells A6, #11, A12 and A8 at depths of 6000'-8000'. The caliper difference was relatively small and subsequent stress analysis revealed that either the breakouts are not stress-induced or the stress state is highly heterogeneous in the region of interest.

Also, Pavel performed analysis of multiple modes of borehole failure for estimation of in situ stress and rock strength (methodology and software development). An integrated methodology was developed to analyze the relationship between the in situ stress and failure of inclined boreholes. Optimally, there is a two-step procedure to apply this methodology in practice: 1) utilize observations of wall failures in inclined holes to constrain the in situ stress and effective rock strength assuming that independent information such as on the least principal stress, pore pressure and overburden is available, and 2) utilize the knowledge on the stress field from the previous step to predict optimal wellbore trajectories and mud weights to stabilize the wellbore.

To implement the methodology starting versions of computer codes were written in MATLAB programming environment. The computations are based on the assumption that the rock is isotropic and it behaves elastically to the point of failure which is controlled by the Mohr-Coulomb criterion. The *GetStress* program computes the orientation and magnitude of the stress tensor (principal stresses are assumed to act vertically or horizontally) from the azimuth of borehole breakouts observed in an inclined borehole and from other a priori information. Regarding this information, there are two modifications: the first concerns the case typical of many sedimentary basins when independent information on Sv, S3 (=Shmin) and Pp is available, and the second is suitable in the case when only Sv is known (Sv=S3 in the reverse faulting stress regime, for example) but the azimuth of SHmax can be a priori estimated. The program may be also used to constrain the rock strength as the conditions for failure are expressed by means of the critical strength C0 and also the breakout width may be taken into account. For the given stress state, the *GetFailure* program computes orientations of compressive and tensile failures in an arbitrarily-oriented borehole and constrains mud weight or effective rock strength required to stabilize the wellbore. Directions of potential breakouts and tensile wall-fractures around holes of various inclinations and azimuths are shown using the "looking down the hole" convention, i.e. as if the reader is viewing the hole by looking down its axis and the breakout azimuth is displayed with respect to the bottom side of the deviated borehole. The *WellboreTrajectory* program also computes orientation and tendency to fail by compressive or tensile failure for the given stress field and borehole orientation but now the stress and hole orientation are functions of depth which makes possible to analyze stability along the whole borehole. Both programs are optimal to design a stable wellbore trajectory from the platform to the target under the assumption that the stress state was determined from observations in the surrounding wells.

Task 4.3.5 - Temperature Mapping

After having established the present-day 3-D temperature distribution in Eugene Island block 330 and the surrounding blocks, Gilles Guerin has isolated the influence of the salt structure on the conductive regime (using a 3-D numerical model of heat conduction, based on the lithology delineated by the 3-D seismics). Once this influence of the salt is removed from the observed temperatures, there is a 5-10^{o} C anomaly following the trend of the red fault in the depth range of the most productive sands. This temperature anomaly is interpreted as the influence of fluids migrating through the fault, and suggests a circulation more active at depth in blocks 338,339, and extending laterally in the fault while migrating upward, filling oil reservoirs in Eugene Island blocks 330, 331 and 314. A first series of 2-D numerical models across the fault shows that short fluid pulses (~ 1000 years) could generate the observed anomalies, but the extent and the duration of the migrations can only be fully apprehended by the 3-D modeling, still to be completed.

Task 4.4 - Amplitude Mapping Analysis

The patent application for 4-D seismic amplitude imaging titled: "4-D Seismic Interpretation and Imaging Utilizing Amorphous Diffuse Intra- and Inter-Period (ADIP) Projectors" is still in development. Albert Boulanger has found significant methodologies to generalize it into a techniques patent that will be more useful to disparate datasets.

A new patent application has been initiated for our Quick Look methodology that now varies enough from the original that a new patent is called for. A patent on the seismic analysis method for multiple seismic surveys was completed and submitted.

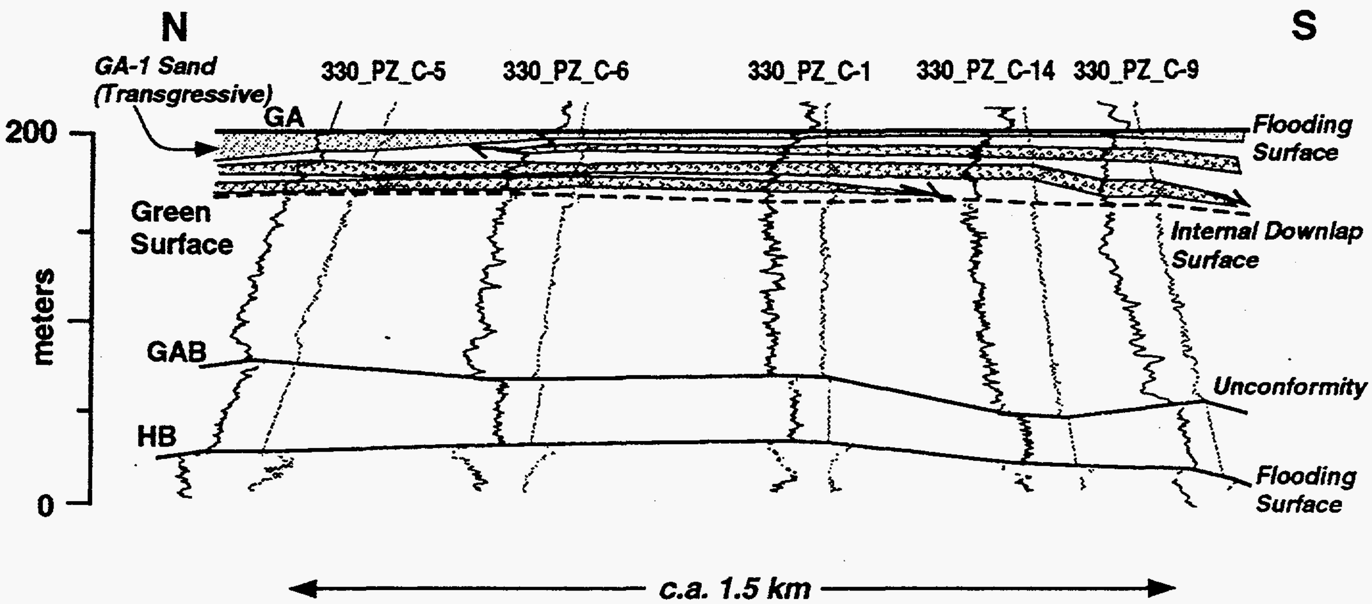

Figure 1: Stratigraphic cross-section showing detailed correlation of charged clean sands 10s of feet thick of the upper portion of the GA-2 sand. The pattern shows transition from channel to deltaic clinoform deposits. Compartmentalization of the reservoir by such depositional features is visible in amplitude anomaly maps of the top of the GA, as well as in production from individual wells.

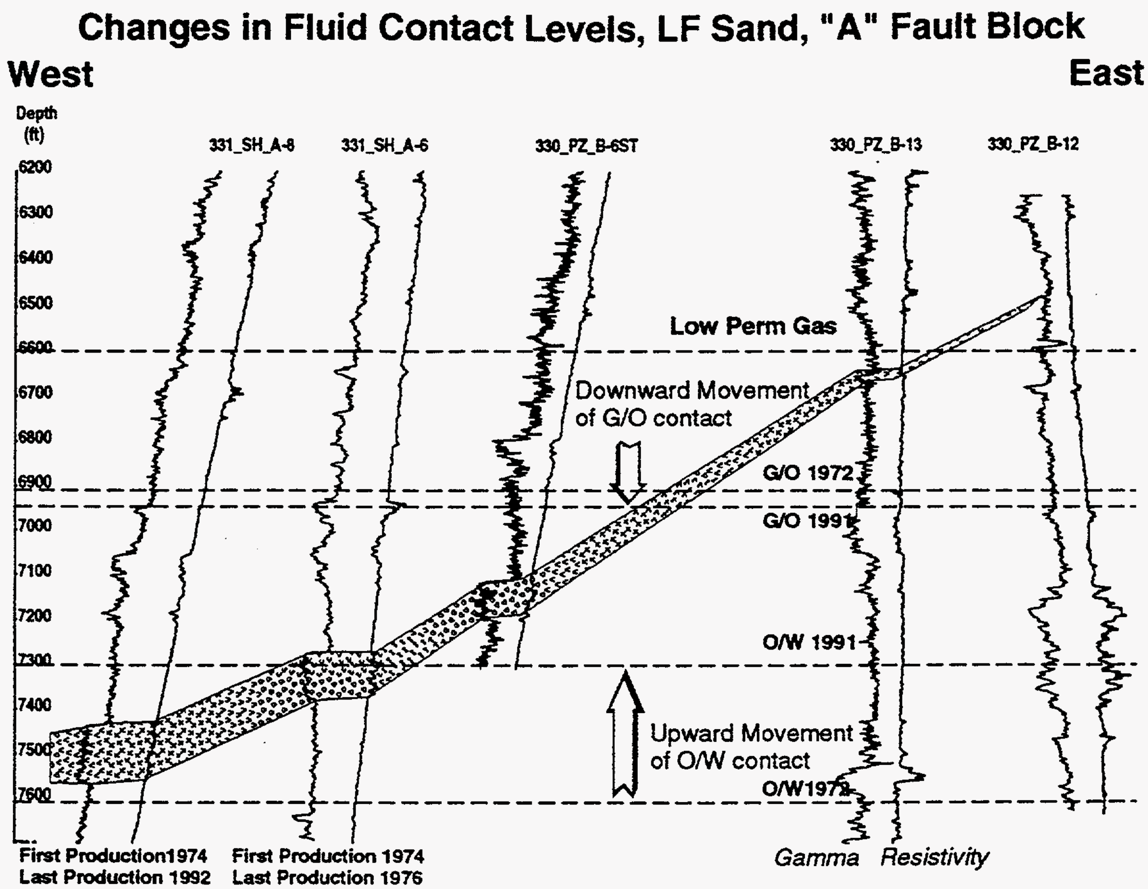

Figure 2: Structural cross-section of LF Sand in "A" fault block showing movement of fluid contacts as inferred from production data.

TASK FIVE

MODELING

Larry Calthes - Cornell
Jeff Nunn - LSU

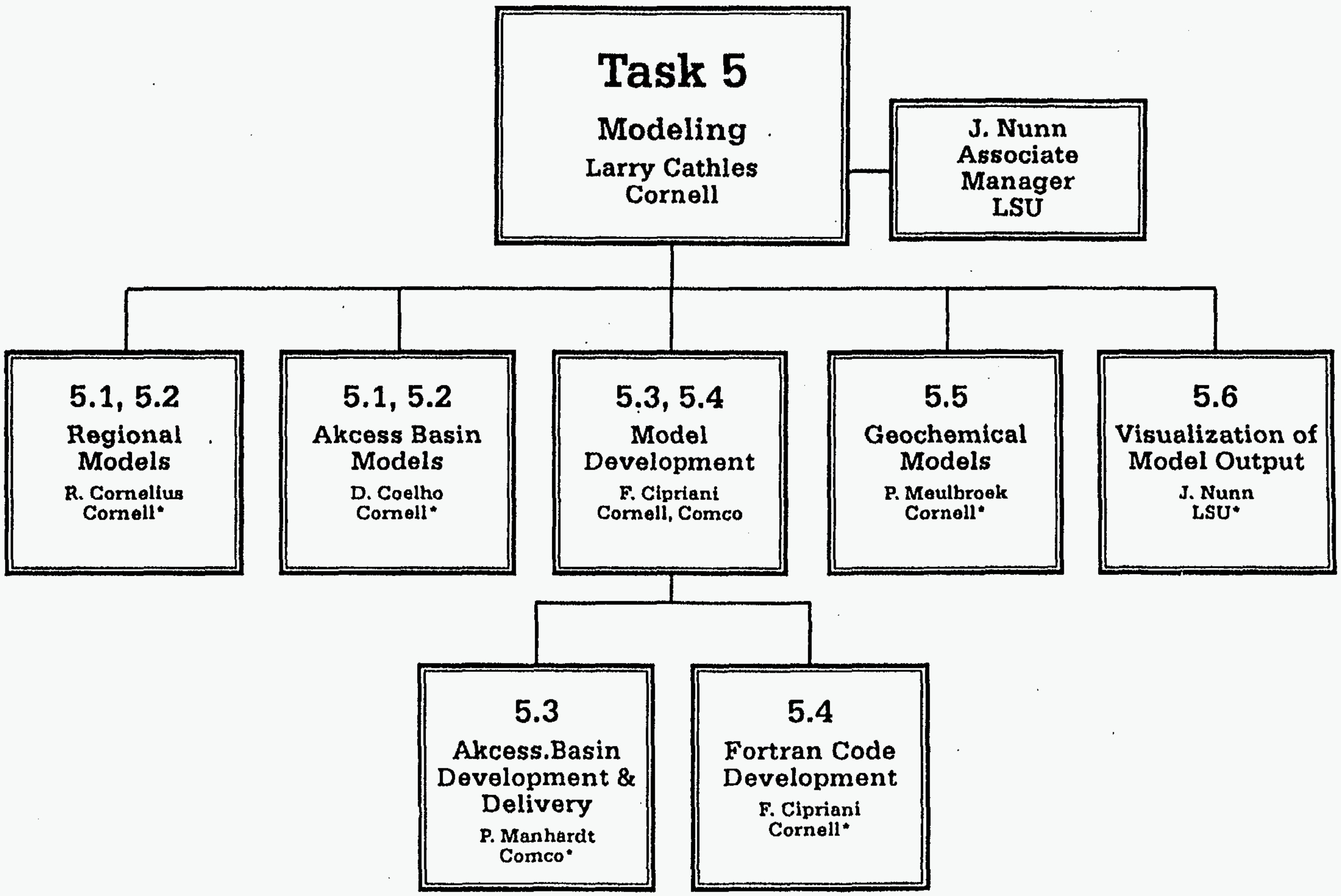
Task 5
Modeling
Larry Cathles
Cornell
J. Nunn
Associate
Manager
LSU
5.1, 5.2
Regional
Models
R. Cornelius
Cornell*
5.1, 5.2
Akcess Basin
Models
D. Coelho
Cornell*
5.3, 5.4
Model
Development
F. Cipriani
Cornell, Comco
5.5
Geochemical
Models
P. Meulbroek
Cornell*
5.6
Visualization of
Model Output
J. Nunn
LSU*
5.3
Akcess.Basin
Development &
Delivery
P. Manhardt
Comco*
5.4
Fortran Code
Development
F. Cipriani
Cornell*

Task 5 - Modeling
Larry Cathles - Task Manager

The pre-processor was modified this quarter to take into account isostasy (which is important on the longer regional lines) and to compute the redistribution of salt in 3D rather than 2D (along a 2D section) only.

Two dimensional models simulating temperature in the SEI minibasin suggest that the distinctive pattern of temperature observed in Block 330 (shallow concave up isotherms underlain by deeper concave down isotherms) can best be explained by the thermally insulating effects of hydrocarbons. Simulation of the movements of low salinity fluids out of the overpressured zone in SEI 330 show that buoyancy effects channel these fluids into high permeability layers in the stratigraphy. Haline convection around salt bodies with complex geometry was simulated. Dramatic flow (both down and up) results wherever there is a gap in salt sills. These results are all highly relevant to interpreting temperature and water chemistry data in the SEI Minibasin.

Akcess.Basin has been modified to include pumping, and the effects of pumping on inducing or restricting flow through a fracture that penetrates into an overpressured zone are being investigated. Also preliminary calculations have been made on the effects on oil recovery of gas exsolution during pumping. These two studies show how spin-offs from the main DOE-funded research could lead to improved production strategies.

Fault plane maps were made of the juxtaposition of sands across the Red fault and F fault in the SEI minibasin. These maps show where flow connections might exist across these faults. Simple model calculations of flow between sands juxtaposed by faulting show that model simulation of Allen-type (e.g., sand to sand) cross fault flow are feasible at least in 2D.

Sections describing a very realistic 3D model of the SEI minibasin have been prepared from an interpretation of the Pennzoil

3D survey. These sections will provide the basis for 3D models of temperature, hydrocarbon generation, and fluid flow in the minibasin that will be carried out this summer.

5.1 Geologic Input

5.1.1 2-D flat files, SEI Minibasin Scale (100% completed)

5.1.2 3-D flat files , SEI Minibasin Scale (100% completed)

5.1.3 Realistic 3-D SEI description (100% completed)

See discussion in 5.2.4.

5.1.4 Present Porosity distribution (90% completed)

All available log data in the SEI Minibasin have been processed. Work is now focusing on visualizing the data in AVS. The modules developed at Lamont are being adapted to this need. Work should be completed next quarter, finishing this task.

5.1.5 Representative Volume Element (RVE) 2-D Seismic Lines (95% Completed)

Mark Rowan's two regional lines have been processed and added to the six previously processed regional Arco lines. The lines will all be reprocessed next quarter to include the new pre-processing additions of 3D salt redistribution and isostasy. See 5.4.1 below.

5.1.6 Near Fault Details (100% Completed)

Very detailed sections incorporating all major individual sand layers and faults have been prepared to provide a basis of 3D modeling (see 5.2.1). Fault plane maps of the juxtaposition of these sands across the A (red) and F faults have been presented and discussed in a Cornell Ph.D. thesis that Laurel Alexander defended this past quarter.

5.1.7 History of Salt Movement (80% Completed)

New pre-processing techniques were developed to extend the algorithm that infers salt redistribution from sedimentation pattern to consider the redistribution in 3D rather than 2D. Isostasy has also been added. Since isostasy provides accommodation space for large scale sediment loading, the need for large salt redistribution to provide space for sediment accumulation is reduced. The algorithms have been successfully applied to the Exxon Louisiana #1 regional line. That analysis shows that space can be provided for the increments of sediment added by isostatic subsidence starting with realistic initial water depths provided the flexural rigidity of the lithosphere is about 10*23 Nm. This rigidity is reasonable and in agreement with literature estimates in the Gulf Coast and glacial uplift estimates in other mature shelf areas such as the North Sea. The new pre-processor developments will require re-processing of the regional lines, but it is anticipated that previous interpretations will not change greatly because these lines are relatively short.

5.1.8 Continuing modification of geologic input (70% Completed)

See above discussion.

5.2 Model Simulations

5.2.1 2-D cross sections for training (100% Completed)

5.2.2 3-D demonstrations (40% Completed)

The pre-processor was extended to include isostasy and 3D salt redistribution. A simple salt-diapirism and extensional faulting example has been prepared for testing the initial 3D models.

5.2.3 3-D realistic SEI simulation (40% Completed)

A very realistic representation of Red Fault and the portion of the SEI Minibasin that abuts it has been made from the Pennzoil 3D seismic survey (see 5.2.4). This will provide the basis for 3D computations to be performed this summer.

5.2.4 Specific Modeling Investigations (50% Completed)

- RVE Modeling

Posters describing salt movement in four Arco regional lines and the two regional lines analyzed by Mark Rowan of Colorado University were prepared and presented in March at the GBRN Booth at the AAPG meeting in Houston.

- Detailed Modeling in the SEI Minibasin; Effects of Salt Diapirism

An 2D analysis of the effect of salt, hydrocarbons and sedimentation rate on temperatures along a NE-SW section across the SEI minibasin suggests that only hydrocarbons can account for the near-surface (to ~2 km depth) temperature anomalies observed there. The insulating effects of the hydrocarbons that fill the reservoir sands mainly on the down thrown side of the Red fault produce concave upward temperature depressions above and concave downward temperature bumps below the reservoirs. This is the pattern observed, and the insulating impact of hydrocarbons appears to be the only feasible way to account for it. The present distribution of salt and the recent pattern of sedimentation appear unable to produce anomalies of the character observed. Bottom hole temperature date was Krieged to define the observed thermal pattern along the computed cross section.

Five very detailed NE-SW sections have been prepared from a detailed interpretation of the Pennzoil 3D seismic survey. These sections describe the throw across the major NE-SW faults in the northern part of the survey as well as the throw across NNW-SSE trending faults such as the Red Fault. The sections will provide the basis for realistic 3D modeling to be carried out this summer.

An extensive set of numerical simulations was run to study how free haline convection beneath an allochthonous salt sheet can give rise to localized salt dissolution. As the salt layer subsides to fill up the empty space created by dissolving salt, a basin-like depression is formed on the top surface of the salt layer. For moderately permeable underlying sediments (vertical permeability 0.1 mD), the resulting rates of salt deformation are comparable to the movement of salt diapirs. Thus salt dissolution could play a role in minibasin formation.

Numerical simulations were run showing how downwelling plumes from the edges of two adjacent allochthonous salt sheets may hydrodynamically interact to produce an upwelling flux of formation water between the two downwelling salty plumes. Expulsion of pore waters from a basin as the result of displacement by the downwelling salt plumes at the edges of a gap in a salt sill is a new mechanism by which fluids can be brought to the near-surface. Unlike the main alternative mechanism, fluid escape from overpressured compartments, this new mechanism can operate under hydropressured conditions.

Simulations of low salinity waters ejected from an overpressured compartment showed a strong tendency to become channelized into high permeability sand layers. Other simulations show that salt dissolution of a salt body will always cause brine to move downward along the flank of the salt. Sand layers in SEI Block 330 host fluids of dramatically different salinity. Variations in salinity may provide information on the history of fluid venting out of overpressure.

- Effects of Gas on Seals and Fluid Flow

An analysis was carried on the impact of gas exsolution on oil recovery. It was shown that if variations in grain size that are known from the literature to occur in 100 md sands occur less than every 14 m of horizontal distance, oil production from the sand body could be significantly affected by gas exsolution after 5 years of pumping. The modeling was based on a "plastic flow" modification to Darcy's Law. The calculations suggested that the most permeable reservoirs would be most affected. This work was supported by matching funds from the Gas Research Institute and is mainly of importance to the DOE project for its implications of how multiphase phenomena might best be modeled on the larger scale in the SEI Minibasin (see 5.3.3).

5.2.5 Model Synthesis (scheduled for initiation 6/1/95)

5.2.6 Final Modeling Assessment (scheduled for initiation 6/1/95)

5.3 Akcess.basin preparation

5.3.1 3-D Template Preparation (100% Completed)

5.3.2 Adaptation of AKCESS.BASIN for parallel execution (90% Completed)

Final tuning will be carried out once 3D models are run.

5.3.3 Two-phase templates (10% Completed)

Stephan Matthai, the Post Doctoral student in charge of this sub-project has announced he will leave at the end of April for Stanford. As a result the thrust of this sub-project will be modified to address particularly the impact of fluid flow in the SEI Minibasin. Modeling will proceed initially at least as described in 5.2.4 above. This modeling approach, although simpler, is probably more fundamental and appropriate to fluid movements in the SEI Minibasin than the more explicit two phase modeling which Matthai planned to carry out. The traditional two phase templates developed last quarter will be tested and applied at a reduced priority and as time permits this summer.

5.3.4 Consultation on and continued tuning of AKCESS.BASIN (40% Completed)

Akcess.Basin 3.2 has been finished, has been installed at Cornell and LSU, and is being installed at Michigan Tech. The Akcess.Basin code has been modified in 2D and 3D to allow addition of new variables in a simple fashion.

5.4 Fortran Algorithms

5.4.1 Diapirism and compaction (100% completed)

Isostasy and 3D salt redistribution were added to the pre-processor that infers salt movements from the sedimentation pattern. Isostasy provides additional accommodation space and can be significant for loads >100 km in size. Three dimensional salt movement means salt may be redistributed from one 2D line in a 3D model to another, and is not constrained to redistribute along each 2D line as was previously the case.

5.4.2 Fault Movement (100% Completed)

Flow between sand layers as they become juxtaposed across a fault was demonstrated in a simple 2D Akcess.Basin test runs this quarter. Results were presented in March to the GBRN/DOE Corporate Affiliates at the semiannual meeting before the AAPG meeting in Houston.

5.4.3 Physical Property Algorithms (100% Completed)

A paper entitled "Using Fabric Theory to Predict Thermal Conductivity in Reservoir Rocks Based on Rock Composition", by M. Luo, J. R. Wood, and L. M. Cathles was published in the Journal of Applied Physics, Volume 32, P. 321-334.

5.4.4 Inorganic Alteration Algorithms (70% Completed)

A C algorithm to compute smectite/illite ratios was developed by M. Luo. Michigan Tech., and transmitted to Cornell for inclusion into Akcess.Basin.

5.5 Chemical Models

5.5.1 Gas solubility and gas generation kinetics (90% Completed)

5.5.2 Inorganic 1D alteration models with gas phase present (70% Completed)

See 5.4.4 above.

5.5.3 Equilibrium inorganic chemical alteration (70% completed)

5.5.4 Isotopic Alteration (10% completed)

5.6 Visualization of Model Output (LSU)

5.6.1 Common Computing Environment (100% completed)

5.6.2 Standardized Input Data File and Macrofile Generation (70% completed)

5.6.3 Visualization and Image Transmission (70% completed)

New methods were developed to transfer images from the GBRN viewer to Macintosh and other platforms as postcript files, for example. An abstract covering this work was submitted to the ARCHIE conference.

Table 1. Revised Gantt Chart for Task 5, Modeling. Entries revised from last quarter are indicated by an asterix (*). Fully completed tasks are indicated by a pound sign (#).

Task #	Name	Start (including the dates)	Finish (including the dates)
5.1	**Geologic Input**	10/1/92	10/31/95
5.1.1	2-D flat files	10/1/92	6/30/93 #
5.1.2	3-D flat files	3/1/93	4/30/94 #
5.1.3	Realistic 3-D SEI description	6/1/93	2/29/95 #
5.1.4	Present Porosity distribution	10/1/92	2/29/95
5.1.5	Representative Volume Element (RVE) 2-D Seismic Lines	10/1/92	2/29/95
5.1.6	Near Fault Details	10/1/93	10/30/95 #
5.1.7	History of Salt Movement	1/1/93	6/30/95
5.1.8	Continuing modification of Geologic input	7/1/94	6/30/95
5.1.9	Geologic and Geochemical observations	4/1/95	10/30/95
5.2	**Model Simulations**	10/1/92	10/30/95
5.2.1	2-D cross sections	10/1/92	6/30/93 #
5.2.2	3-D demonstrations	2/1/93	6/30/95 *
5.2.3	3-D realistic SEI simulation	8/1/93	8/31/95 *
5.2.4	Specific Modeling Investigations	1/1/94	10/30/95 *
5.2.5	Model Synthesis	6/1/95	10/30/95
5.2.6	Final Modeling Investigations	6/1/95	10/30/95
5.3	**Akcess.basin preparations**	10/1/92	6/30/95
5.3.1	3-D template	10/1/92	12/31/94 #
5.3.2	Adaptation of Akcess.basin for parallel execution	3/1/93	2/29/95
5.3.3	Two-phase templates	7/1/93	10/30/95 *
5.3.4	Consultation and continued tuning of Akcess.Basin	2/28/94	6/30/95

5.4 Fortran Algorithms		10/1/92	3/31/95
5.4.1	Diapirism and Compaction	10/1/92`	12/31/94
5.4.2	Fault Movement	2/1/93	12/31/94
5.4.3	Physical Property Algorithms	10/1/93	3/31/95
5.4.4	Inorganic Alteration Algorithms	4/1/94	1/31/95
5.5 Chemical Models		10/1/92	2/28/95
5.5.1	Gas solubility and generation kinetics	10/1/92	4/30/95
5.5.2	Inorganic 1D alteration models with gas phase present	6/30/93	4/30/95
5.5.3	Equilibrium inorganic chem. alteration	10/1/92	6/30/95
5.5.4	Isotopic Alteration	7/1/94	6/30/95
5.6 Visualization of Model Output		1/1/93	10/30/95
5.6.1	Common Computing Environment	1/1/93	9/30/93 #
5.6.2	Standardized Input Data File and Macrofile Generation	1/1/93	10/31/95
5.6.3	Visualization and Image Transmission	1/1/93	10/31/95

Papers Published:

1. M. Luo, J. R. Wood, and L. M. Cathles, 1994, "Using Fabric Theory to Predice Thermal Conductivity in Reservoir Rocks Based on Rock Composition", Journal of Applied Physics, Volume 32, P. 321-334.

Papers Submitted:

1. Sarkar, A. and Nunn, J., 1995, "Free haline convection beneath allocthonous salt sheets: an agent for salt tectonics and fluid flow in Gulf Coast sediments", 16 th Annual Gulf Coast Section SEPM Research Conference.

Meeting Abstracts:

1. Nunn, J. A., Roberts, S. J., Anderson, R. N., Cathles, L. M., and the Global Basin Research Network, 1995, "Visualization technology to find and develop more oil and gas, ARCHIE Conference, May 14-18, The Woodlands, Texas.

Theses Completed:

1. Alexander, Laurel, 1995, Geologic Evolution and Controls on Fluid Flow of the Eugene Island Block 300 Minibasin, Offshore Louisiana, Gulf of Mexico, Cornell PhD Thesis, 206p.

TASK SIX

GEOCHEMISTRY

Steven Losh - Cornell

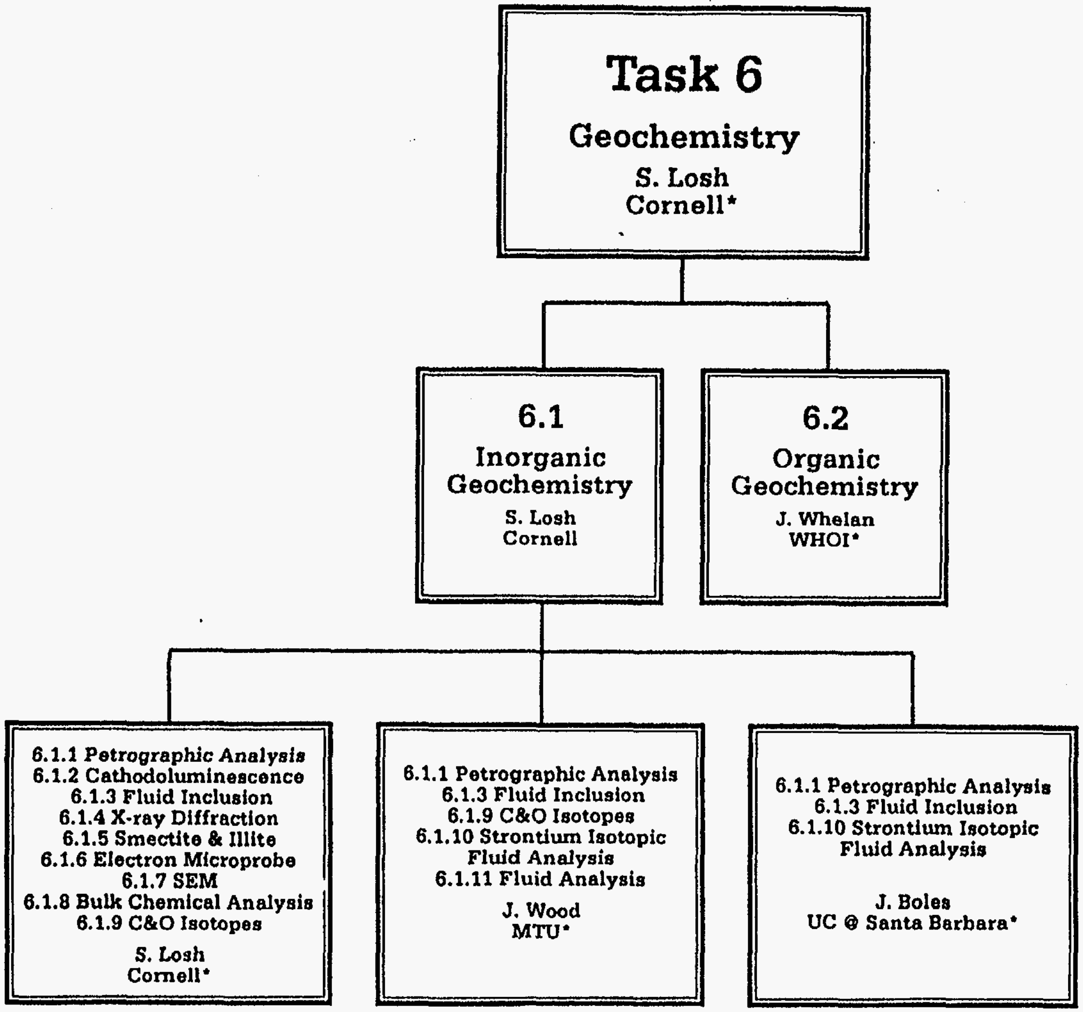
Task 6
Geochemistry
S. Losh
Cornell*
6.1
Inorganic Geochemistry
S. Losh
Cornell
6.2
Organic Geochemistry
J. Whelan
WHOI*
6.1.1 Petrographic Analysis
6.1.2 Cathodoluminescence
6.1.3 Fluid Inclusion
6.1.4 X-ray Diffraction
6.1.5 Smectite & Illite
6.1.6 Electron Microprobe
6.1.7 SEM
6.1.8 Bulk Chemical Analysis
6.1.9 C&O Isotopes
S. Losh
Cornell*
6.1.1 Petrographic Analysis
6.1.3 Fluid Inclusion
6.1.9 C&O Isotopes
6.1.10 Strontium Isotopic Fluid Analysis
6.1.11 Fluid Analysis
J. Wood
MTU*
6.1.1 Petrographic Analysis
6.1.3 Fluid Inclusion
6.1.10 Strontium Isotopic Fluid Analysis
J. Boles
UC @ Santa Barbara*

systematic changes in detrital or diagenetic mineralogy were noted with depth in the wells nor in comparison between wells.

Diagenetic smectite and illite are the most abundant authigenic phase but even these minerals do not exceed 10% by volume in the samples. The clays occur as thin rims on detrital grains and as a pore-filling cement. In many cases, diagenetic clay appears admixed with detrital clay matrix and it is difficult to distinguish the detrital from the authigenic phase. The samples with the most abundant, what is clearly authigenic clay, are B16@5074' which has up to 10% of small scattered lath-shaped birefringent illitic clay particles. Curiously, these crystals are length fast, whereas typical illite is length slow. Other examples of diagenetic clay are in the A19ST well where a birefringent (illitic?) clay forms thin rims about detrital grains or in some cases, pores are partially filled with a yellowish-green to yellowish-grown clay.

Diagenetic carbonate occurs in trace amounts in some samples. Typically it occurs as scattered subeuhedral to euhedral grains or in some cases as grain coatings. In some cases, such as B3ST @5917' and 5930', the yellowish-brown color or the carbonate indicates it is probably siderite. Similar appearing siderite is found in Cretaceous sands from the Alaska North Slope and in this case they can be shown to have formed near the sediment-water interface.

Syntaxial quartz overgrowths are very rare in these samples, indicating that they have not undergone silica cementation due to upwelling hot fluids. The few samples with quartz overgrowths occur as incipient syntaxial overgrowths on a few grains in a few samples. The rarity of the overgrowths indicates that they could be reworked.

Feldspar diagenesis is a sensitive indicator of changing burial conditions. Neither dissolution of feldspar nor insitu albitization of detrital plagioclase can be demonstrated in these samples. Albitized feldspar occurs in the samples but is is in a mixed population with fresh plagioclase. This suggests that albitization is not an insitu process. In addition, zoned plagioclase, typically some of the most unstable feldspar, appears unaltered.

In summary, these samples are not extensively cemented. Clay minerals, which appear to be the dominant diagenetic phase, appear similar to those found in incipient diagenesis. The most compelling evidence for upwelling hot fluids from deep in the basin would be the presence of abundant authigenic silica. Such evidence is not found in these "GA" sand samples."

Diagenesis of the 70 examined HB sand samples (wells B16, B3ST, A7ST, C15ST, C13, C11, C9, C21, C2, #3, #4 (A1), A23, A19ST, C20, A6ST, A13, B12, C3, #1, #6) is largely similar to that observed in the GA sand, except that carbonate (both detrital and authigenic) is slightly more abundant, and that albitization of plagioclase is more common, in some cases involving all of the plagioclase in a sample (particularly samples from C2, C9, and C13). In at least one case (B16, 6144'), albitization is inversely correlated with carbonate cement: where cement is abundant, feldspars are fresh, whereas uncemented zones contain albitized plagioclase. This type of relationship indicates the albitization is in situ, and that the carbonate cement in this sample predates albitization. Pronounced variations in proportion of albitized grains to unalbitized ones exist over short vertical distances in the wells; . Intergrown fine-grained calcite and dolomite were noted in two samples from the B16 well; these were analyzed for carbon and oxygen isotopic composition (6.1.9). Preliminary plotting of these diagenetic indicators on a map shows little to no apparent relationship between extent of diagenesis and proximity to faults; however, samples above the Oil/water contact on the north side of a nearly east-west fault traversing the southern part of Block 330 have more carbonate cement and a higher proportions of albitized to unalbitized plagioclase grains than do samples south of this fault or samples below the O/W contact. There does not appear to be any correlation between abundance of albitized grains or authigenic carbonate and stratigraphic position within the HB "sand". More work is being done to assess the possibility of in situ albitization; if such a process were occurring, it would be unusual given the relatively low temperature of the HB sand. Albitization generally begins at about 80-100 C, whereas the HB sand is at temperatures closer to 60 C. Sodium depletions relative to chloride in brine samples have been noted by Lynn Walter (Univ. Michigan), raising the possibility that, if albitization is an in situ process in these rocks, it may have a chemical rather than a thermal cause.

Vitrinite reflectance measurements have been performed by Lorraine Eglinton at Woods Hole on cuttings from fault intercepts in Block 330 (Table 1), as well as on sidewall cores above the fault intercepted in the A6ST well (Table 2). Cuttings were obtained for intervals identified on Pennzoil marked logs as being where the 'A' fault was intersected; typically, two contiguous 30-foot intervals were analyzed (figures 1 through 7). These analyses were done as a reconnaissance of the fault in order to highlight wells where more data should be obtained. Most washed cuttings are heavily contaminated by drilling introduced artifacts and lithologic fragments are present in only trace abundances. The cuttings were generally of poor quality as regards organic content, but yielded results that, if taken with adequate caution, may indicate that much of the main growth fault in Block 330 is a paleothermal anomaly. If the data are interpreted straightforwardly, the "strength" of the anomaly decreases almost monotonically from northwest to southeast in Block 330; the Pathfinder Well penetrated the lone known "cold spot" in the fault (although other such spots may in fact exist). At all other locations, the fault zone reflectances are higher than in samples well outside the fault zone at comparable depths, although the distinction diminishes to the southeast.

Tmax, measured on the same samples as analyzed for vitrinite reflectance, is a thermal maturity parameter derived from pyrolysis and represents the temperature of maximum generation of hydrocarbons from kerogen. Lithologic fragments were carefully picked and crushed for pyrolysis. Like the Vitrinite reflectance measurements, the Tmax data also show scatter. There are often multiple lobes on the P2 peaks and both Tmax peak1 and peak2 are shown in Table 1. The lobes may indicate the presence of asphaltic, polar material. This material often affects Tmax by shifting it to higher values if the material is a late asphaltene precipitate and to lower values if it is an, early sulfur rich species. The Tmax data are given in Table 1, in figures 2-7 and pyrograms are shown for well C7 in figure 8. The better quality samples provide better data, particularly so for samples from well C7 (figure 8). While there does not appear to be major shifts in Tmax there is an elevated P1 peak in the sample from 5650 - 5680 ft. that indicates greater abundances of migrated hydrocarbons near the upper faulted zone. Maturity determinations for Type III organic matter support vitrinte reflectance data.

Sidewall cores above the fault in the A6ST well (Table 2)were analyzed at WHOI in order to ascertain whether previously-reported anomalously high vitrinite reflectances in fault zone samples were in fact related to the fault zone and, if so, what the geometry of the fault zone paleothermal anomaly looks like. Nearly all available sidewall cores (seven in all) above the fault were analyzed; in most cases, polished plugs, thin sections, and impregnated mounts were made from the same samples in order to compare techniques. As indicated in Table 1, average reflectance decreases sharply with increasing distance above the fault; extrapolation of a best fit line through these points intersects the "normal" profile, comparable to that determined for the Pathfinder well, at about 6900 feet (depth to top of fault is about 7230). Thus, the "thermal halo" above the fault in this well is about 300 feet wide, or about 225 feet measured perpendicular to the fault. By way of comparison, the oxygen and carbon isotopic depleted zone is about 100 feet wide, centered on the top of the fault (see DOE Annual Report).

Vitrinite reflectance was measured on cuttings from the Pathfinder well, below the bottom of the cored interval (table 1). These %Ro values are slightly higher and show somewhat more scatter than values measured in the core or in sidewall cores.

6.1.4., 6.1.8. Exxon Production Research personnel have expressed interest in comparing chemical effects of fluid flow in the A6ST well, and have undertaken X ray diffraction analysis of ten sidewall core samples showing varying degrees of deformation. Splits of the same samples have been sent to X Ray Assay Labs for bulk chemical analysis. Splits have also been prepared for stable isotopic analysis, and we are awaiting results from EPR's x-ray work prior to sending these samples off.

6.1.9. Stable isotopic analysis. Three samples of intergrown calcite+dolomite from the HB sand were analyzed by timed extraction: gas was collected at 20 minutes and 3 hours after initiation of the reaction with phosphoric acid. The 20-minute isotopic value is taken to represent calcite; the 3-hour value is taken to represent dolomite (table 3). Straightforward application of Sheppard and Schwarcz's calcite-dolomite isotopic thermometer gives temperatures between 80 and 130 C, considerably hotter than ambient temperatures. Although the two phases appear to be in textural equilibrium, the values may lie on a mixing line between pure calcite and dolomite end members, such that the calculated fractionations between these phases are less than they really are, leading to an over-estimate of temperature. The calcite d18O value is compatible with equilibration with water at about 50 C. The positive d13C values indicate absence of organically derived carbon in the waters with which these minerals equilibrated.

6.1.11 Brine analysis. Interpretation of brine chemistry is being carried out by Prof. Lynn Walter, Univ. of Michigan, and Jim Wood, MTU. The MTU report is as follows; the figure is not included.

Work on this subtask consisted of interpretation of the water data in preparation for the final report this fall. Dr Lynn Walter (U Michigan) attended the annual GBRN meeting in Houston and presented her interpretations of the data. Subsequently she spent 2 days at USF with Dr. Wood discussing the data and how best to interpret them.

It is clear that the bulk of the dissolved solids at Eugene Island are derived by dissolution of halite, followed by alteration by interaction with the host rocks...The data [in the figure] are sorted by Na+ concentration. Two features stand out: (1) Na+ is by far the dominant cation and the samples can be split into two groups based on Na+ concentrations and (2) the rest of the major cations (K+, Ca++, Mg++) are subordinate to Na+ in all samples with nearly constant relative proportions. The divide based on Na+ concentration occurs at approximately 1.5 molal and generally includes all samples collected from the HB, OI, and J horizons. The more concentrated fluids were collected from the GA, L, and MG horizons and are significantly higher in total dissolved solids, ranging between 2 and 2.4 molal.

We interpret these waters as having evolved through three major steps: (1) development of a concentrated brine through dissolution of halite followed by (2) mixing this brine with more dilute waters, probably sea water in the present formations, and (3) chemical interaction between the brines with the host rock to exchange Na+ for Ca++ and Mg++. Potassium plays a minor role. It is not clear that step (3) followed (2): it could well be that the concentrated brine was altered prior to mixing with sea water and injection into the present horizons.

Work is continuing on the interpretation of these brines, with emphasis on the fluid rock interactions and the possible mechanisms that could account for the elevated calcium concentrations. The strontium isotope data should be of value in this."

Task 6.2 Organic Geochemistry

Revised Statement of Work: Woods Hole Oceanographic Institution

We have requested a no cost extension of our subcontract to Oct 31, 1995 because of the late start of the Woods Hole subcontract, in order to complete our Statement of Work according to schedule outlined below:

Task 6.2.1.d Hydrous pyrolysis, completion of experiments on rates of oil cracking to gas using oil-permeated Pathfinder cores (experimental work begun; anticipated completion: 7/31/95)

Task 6.2.2.b: Completion of biomarker and gas analyses of Pathfinder cores and oils (analyses are in progress; anticipated completion date analytical work: 8/31/95).

Task 6.2.3a: Work is in progress on a paper on relation of Pathfinder oils to other EI-330 oils by Dr Rick Requejo of Texas A & M. Anticipated completion: 8/31/95

Task 6.2.3a: Placing organic geochemical data into 3-D geological framework now available from completed Lamont and Penn State Pathfinder work. To extent possible, place constraints on permeability paths and barriers in EI minibasin by combining organic geochemical data and thesis work of Laurel Alexander. Write preliminary manuscipt on results (Work is just beginning now that Pathfinder volume is complete. Anticipated completion: October 31, 1995)

Task 6.1 and 6.2.3: Write paper summarizing vitrinite reflectance and inorganic geochemical data for zones of abnormal heating in EI-330 (Lorraine Eglinton, with Steve Losh; work in progress; anticipated completion July, 1995).

Task 6.2.3.b: Complete hydrous pyrolysis paper - kinetics and estimation of amount of gas available to drive fluid flow processes in EI-330. Completion of hydrous pyrolysis paper. Requires data from Task 6.2.1.d above. (Anticipated completion: October 31, 1995)

Progess during this quarter:

Task 6.2.2, oil, gas, and kerogen analyses:

1) HRGCMS analyses:

a) Set up instrument to search oils for carbazoles. Determined that there are none of these in the Eugene Island oils analyzed to date, so deleted this analysis from our work proposal.
b) Analytical work completed on EI oil analyses; peak identification and data manipulation and storage is in progress.

2) Completion of kerogen and pyrolysis analyses on Pathfinder and adjacent well kerogen (see attached report)

Task 6.2.3, Organic geochemistry, Modeling and technology transfer:

3) Final publication of two papers occurred during this quarter:
a) Paper on organic geochemistry of Pathfinder Well oils on CD-ROM volume.

b) J.K. Whelan, M.C. Kennicutt II, J.M Brooks, D. Schumacher, and L.B. Eglinton (1994) Organic geochemical indicators of dynamic fluid flow processes in petroleum basins. Advances in Organic Geochemistry 1993, Organic Geochemistry, v. 22, pp 587-615.

4) In process of putting all of geochemical data into data base so that it will be publicly available via STP through Mosaic Program on Internet

Table 2. Vitrinite reflectance measurements, A6st well.

Well	Depth (MD)	%Ro	No.	S.D.	Sample type
A6ST	5801		0	0.00	VR Block
A6ST	5801	.40	1	0.00	Thin Section
A6ST	5803	.48	6	.05	Sidewall
A6ST	5803		0	0.00	Thin Section
A6ST	6233	.32	1	0.00	VR Block
A6ST	7104	.43	2	.18	Sidewall
A6ST	7104	.44	3	.05	Thin Section
A6ST	7107	.49	5	.10	Thin Section
A6ST	7107		0	0.00	VR Block
A6ST	7114	.40	4	.08	Sidewall
A6ST	7114	.47	6	.07	VR Block
A6ST	7114	.45	3	.14	Thin Section

A6ST	7269	.43	5	.14	Sidewall
A6ST	7269	.49	4	.06	Thin Section
A6ST	7279	.54	1	0.00	Sidewall
A6ST	7279	.52	3	.07	Thin Section
A6ST	7283	.45	10	.06	Thin Section
A6ST	7289	.45	18	.07	VR Block
A6ST	7327	.58	22	.05	VR Block (old meas.)
A6ST	7340	.55	13	.11	VR Block (old meas.)
A6ST	7344	.54	13	.13	VR Block (old meas.)
A6ST	7348	.53	18	.04	VR Block (old meas.)
A6ST	7440	.54	13	.08	VR Block (old meas.)

Table 3. Carbon and oxygen isotopic analysis of carbonates

Sample	Mineral	d13C(PDB)	d18O(SMOW)
B16/6140-1	calcite	+0.4	23.3
	dolomite	+1.9	26.6
B16/6140-2	calcite	+0.5	23.1
	dolomite	+1.3	26.0
B16/6144	calcite	+0.3	23.4
	dolomite	+1.0	26.0

Table 1

Table 1. Vitrinite and Pyrolysis Tmax data

Well Name	Composite Depth Range (feet)	Top Measured Depth (feet)	Bottom Measured Depth (feet)	%Ro*	# Readings	Sd.	Tmax RockEval equivalent** Peak 1 (°C)	Tmax RockEval equivalent Peak 2 (°C)
#5	30	6850	6880	0.41	4	0.05	427.727	
#5	30	6880	6910	0.38	1	0	408.235	539.409
#5		6910	6940				482.111	
#7	30	6620	6650	0	0	0	469.606	
#7	30	6650	6680	0.37	1	0	441.444	487.227
#7	30	6680	6710	0.27	2	0	416.432	468.494
#7	30	6710	6740	0.45	2	0.05		
C7	30	5650	5680	0.51	2	0	417.414	
C7	30	5680	5710	0.45	6	0.05	395.362	
C7	30	5980	6010	0.48	1	0	430.389	
C7	30	6010	6040	0.44	5	0.07	427.055	
A16	30	5450	5480	0.55	2	0		404.484
A16	30	5480	5510	0.46	2	0.07		419.756
A16	30	5510	5540				283.468	407.577
A20S/T	30	8090	8120	0.31	3	0.13	341.355	
A20S/T	30	8150	8180				345.98	526.131
A20S/T	30	8210	8240					411.537
A20S/T	30	8270	8300	0.34	7	0.09		458.392
A20S/T	30	8330	8360	0.47	2	0.01	298.067	537.354
A20S/T	30	8330	8360				290.166	542.668
A20S/T	30	8360	8390	0.37	3	0		507.107
A20S/T	30	8390	8420					475.527

@ 23°C), 546nm, x40 objective, Zeiss microscope

m CDS pyrolysis Tmax (°C)

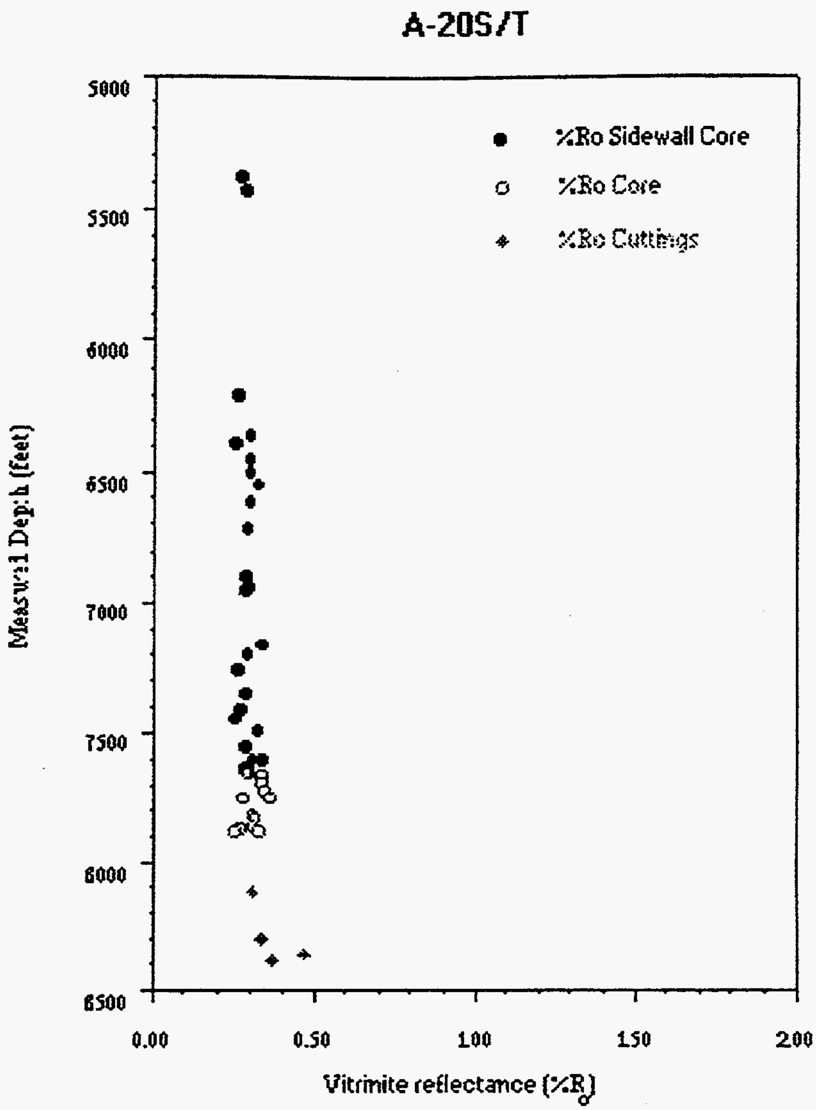

Figure 1: Vitrinite reflectance for cores, sidewall cores and cuttings samples from EI-330, well A-20 S/T (Pathfinder).

Well A-20 S/T (Pathfinder) Vitrinite Reflectance

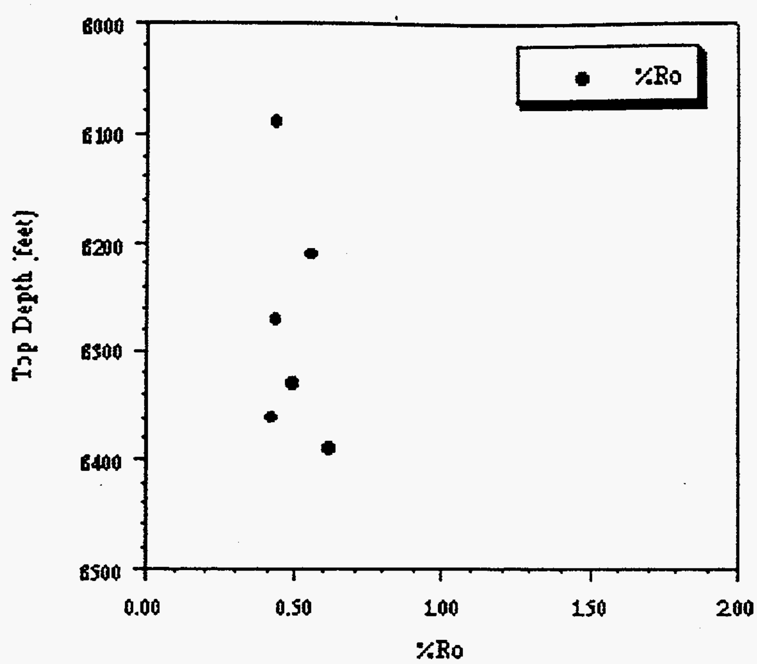

Vertical bars indicate depth range

Well: A-20 S/T Tmax (IC)

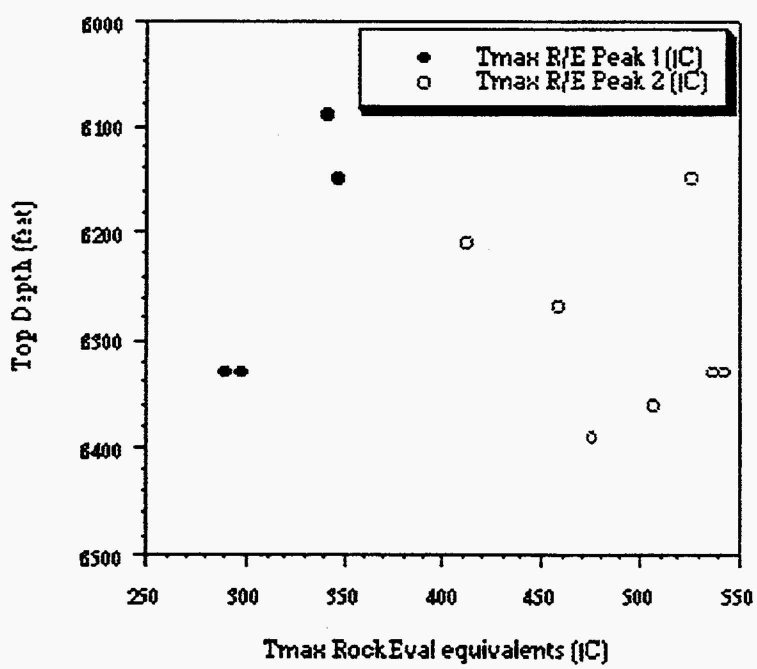

Vertical bars indicate depth range

Figure 2: Vitrinite reflectance and Pyrolysis Tmax plots for EI-330, well A-20S/T.

Well C-7 Vitrinite Reflectance

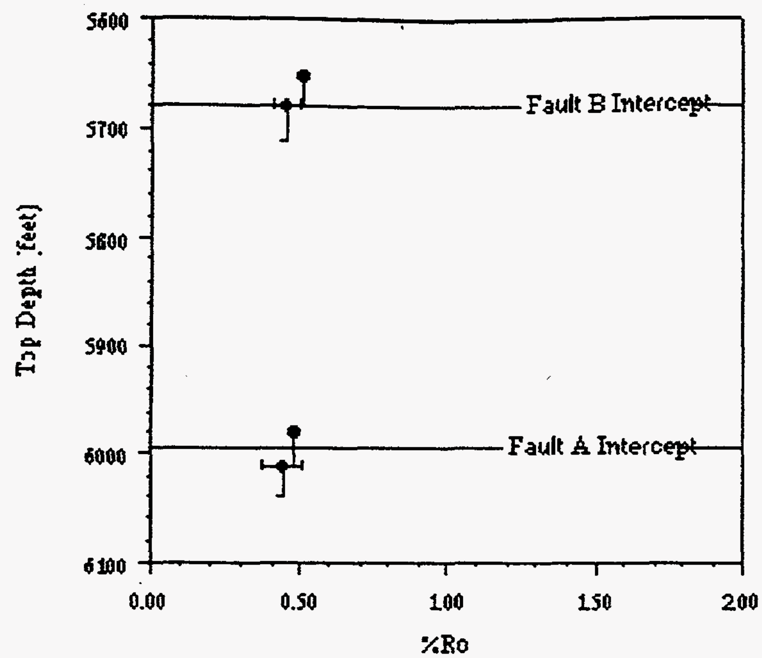

Vertical bars indicate depth range

Well: C-7 Tmax

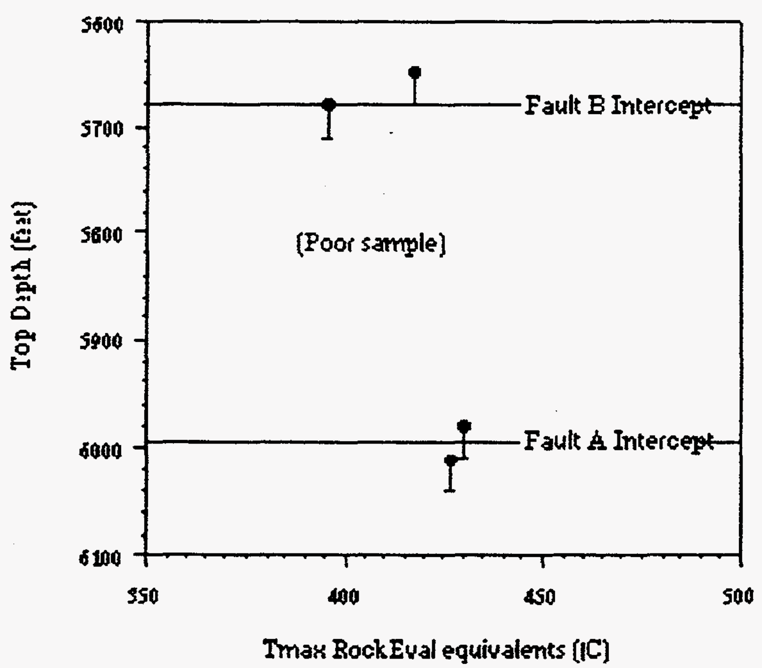

Vertical bars indicate depth range

Figure 3: Vitrinite reflectance and Pyrolysis Tmax plots for EI-330, well C7.

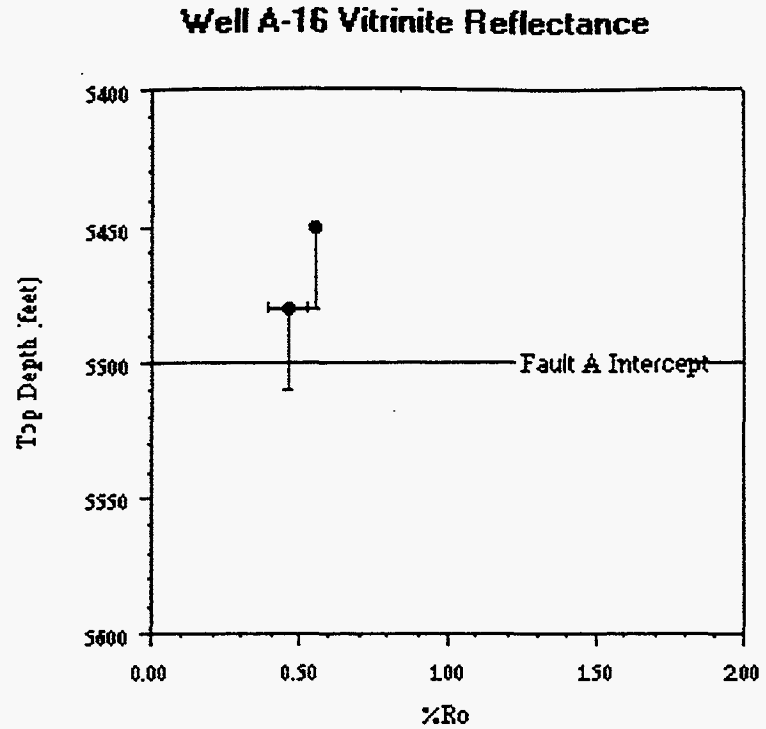

Vertical bars indicate depth range

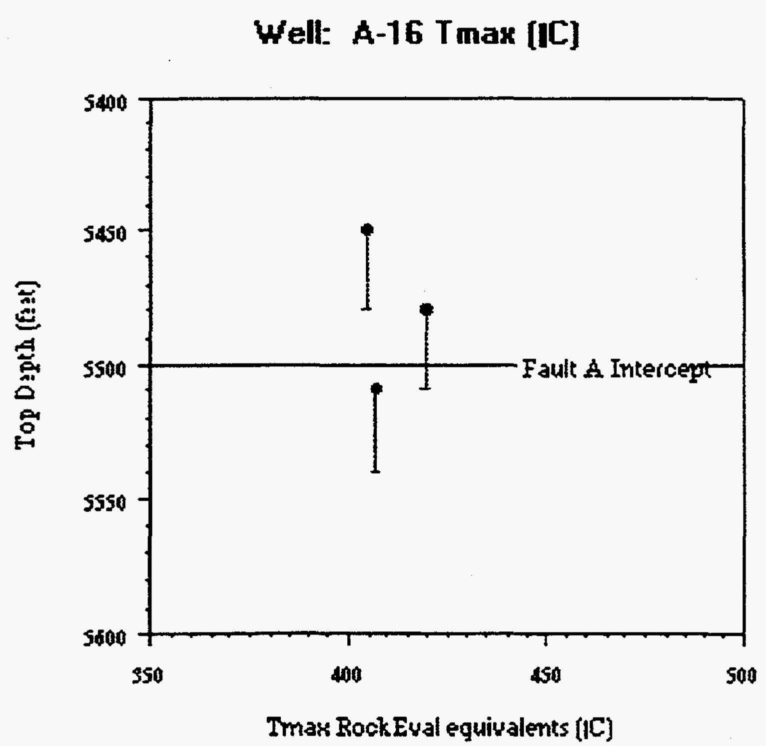

Vertical bars indicate depth range

Figure 4: Vitrinite reflectance and Pyrolysis Tmax plots for EI-330, well A-16.

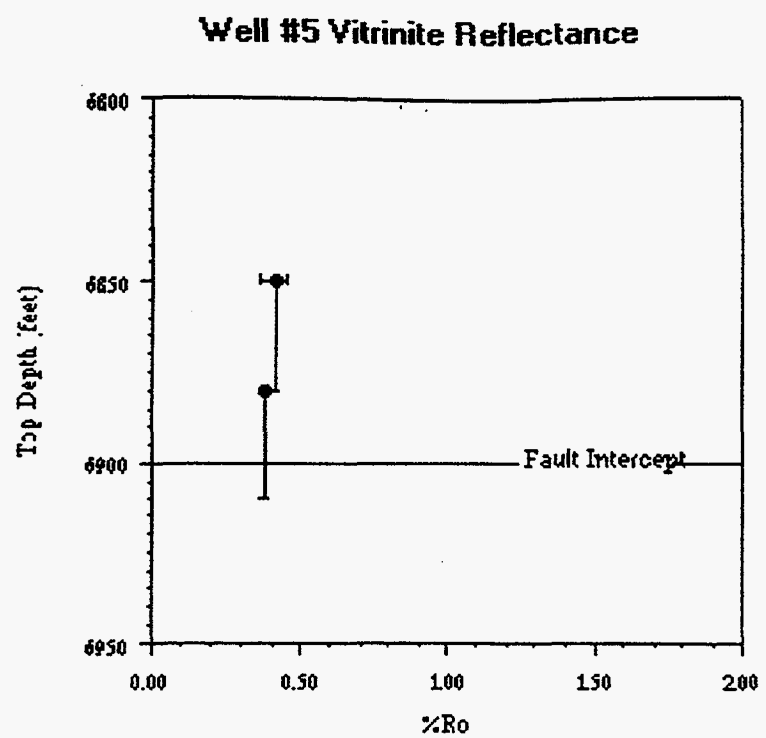

Vertical bars indicate depth range

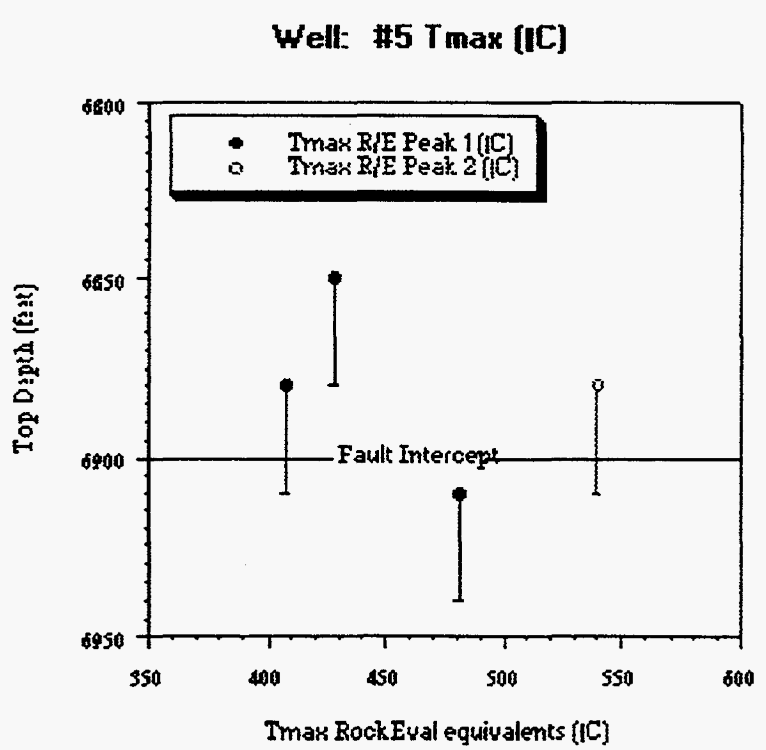

Vertical bars indicate depth range

Figure 5: Vitrinite reflectance and Pyrolysis Tmax plots for EI-330, well #5.

Well #7 Vitrinite Reflectance

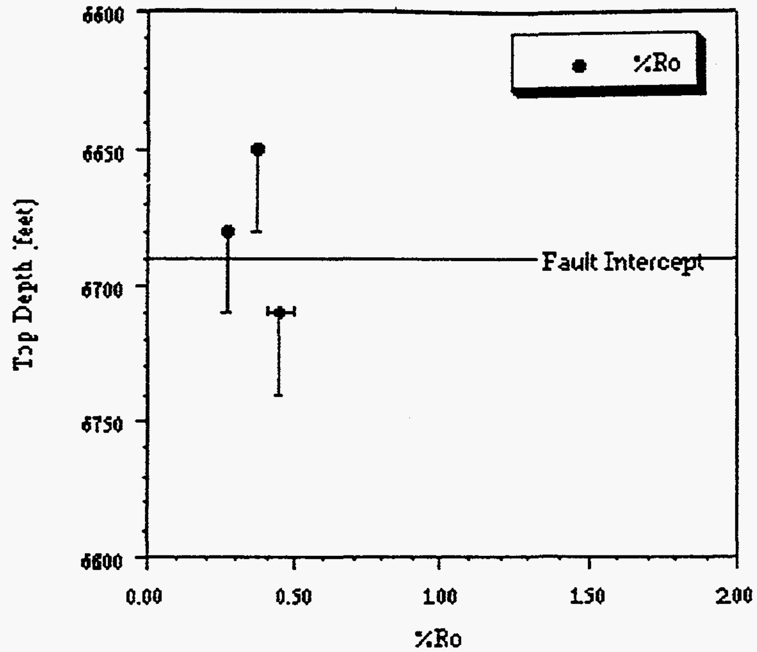

Vertical bars indicate depth range

Well: #7 Tmax (C)

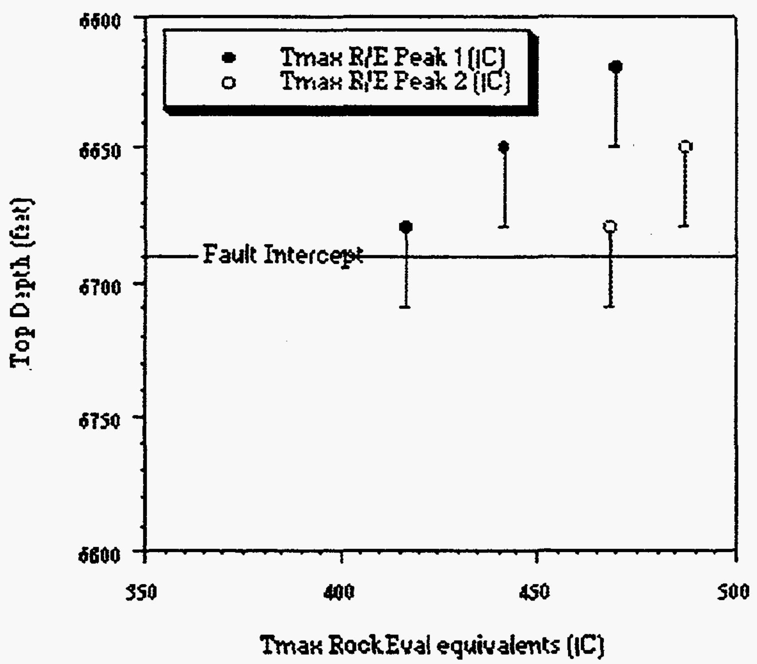

Vertical bars indicate depth range

Figure 6: Vitrinite reflectance and Pyrolysis Tmax plots for EI-330, well #7.

Well A-5 Vitrinite Reflectance

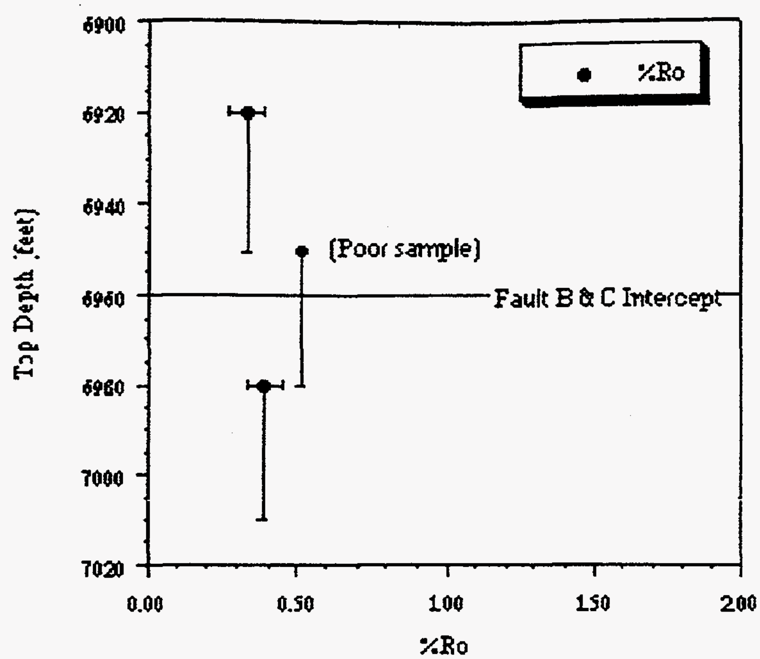

Vertical bars indicate depth range

Well: A-5 Tmax (°C)

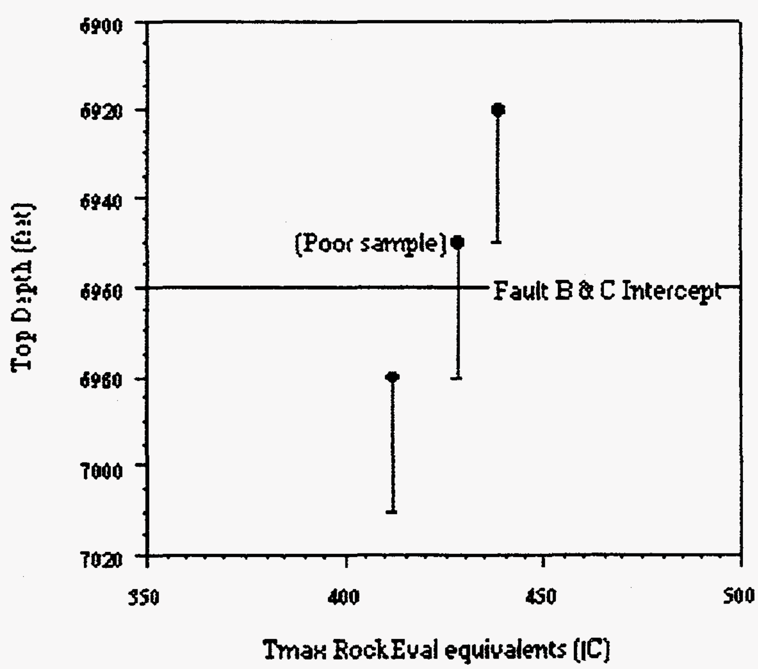

Vertical bars indicate depth range

Figure 7: Vitrinite reflectance and Pyrolysis Tmax plots for EI-330, well A-5.

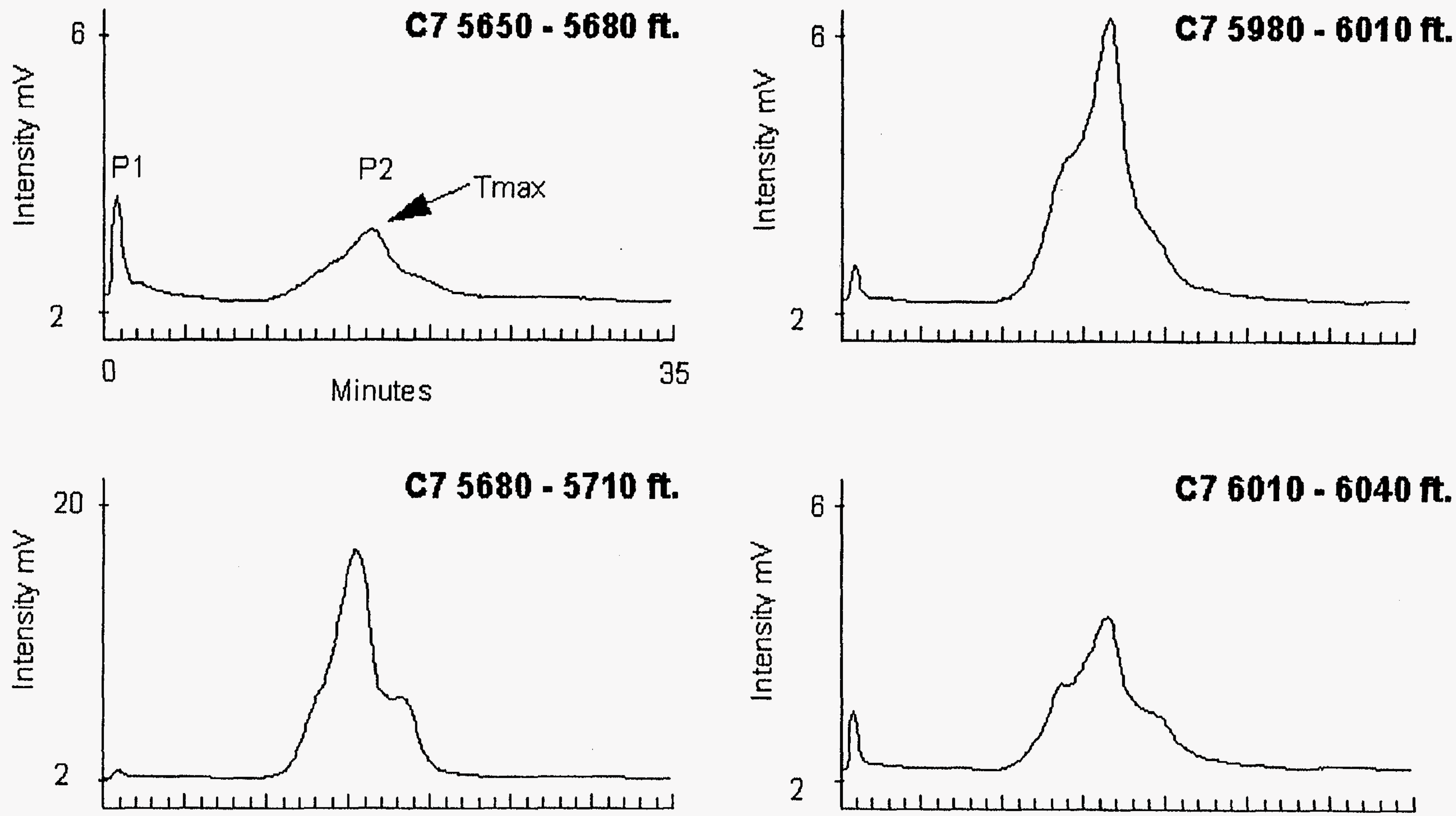

Figure 8: Pyrograms for EI-330, well C7. The sample at 5650 - 5680 ft. has enhanced P1 relative to P2 indicating a higher abundance of migrated hydrocarbons relative to deeper samples in this well.

TASK SEVEN

DATA

INTEGRATION

Roger N. Anderson
LDEO

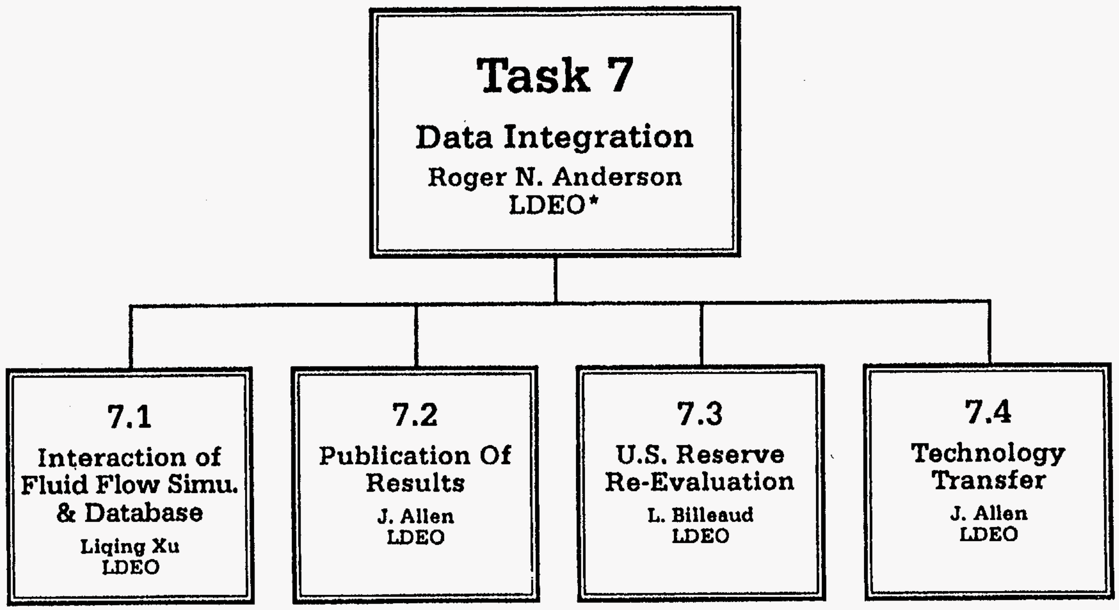
Task 7
Data Integration
Roger N. Anderson
LDEO*
7.1
Interaction of Fluid Flow Simu. & Database
Liqing Xu
LDEO
7.2
Publication Of Results
J. Allen
LDEO
7.3
U.S. Reserve Re-Evaluation
L. Billeaud
LDEO
7.4
Technology Transfer
J. Allen
LDEO

Task Seven - Technology Transfer
Roger N. Anderson - Task Manager

<u>OBJECTIVES:</u> The purpose of this task is to integrate all results into one comprehensive perspective of the project's objectives and to transfer the results to industry. This will involve the interactions between the various project task outputs and the transfer and dissemination of the major conclusions of the study.

<u>SUMMARY OF TECHNICAL PROGRESS:</u>

7.1 <u>Interaction of Fluid Flow Simulation & Database:</u> Once the model results become predictive, this information will be made part of the permanently maintained, on-line geological database, World Wide Web, currently available over Internet.

7.2 <u>Publication of Results:</u> The following papers were published and abstracts presented in the first quarter of 1995 or were left previously unreported to the DOE.

Publications and Abstracts in the first quarter of 1995:

1. Anderson, R.N., A. Boulanger, W. He, Y.F. Sun, L. Xu, D. Sibley, J. Austin, R. Woodhams, R. Andre, and K. Rinehart. 1995. "Method Described for Using 4D Seismic to Track Reservoir Fluid Movement" <u>Oil & Gas Journal.</u> (April 3): pp. 70-74.

2. Anderson, R.N., W. He, Y.F. Sun, L. Xu, D. Sibley, J. Austin, R. Woodhams, R. Andre, and K. Rinehart. 1995. "4D Seismic Helps Track Drainage, Pressure Compartmentalization." <u>Oil & Gas Journal.</u> (March 27): pp. 55-58.

3. Anderson, R. N., L.B. Billeaud, P.B. Flemings, S. Losh, J.K. Whelan, and the Global Basins Research Network. 1995.

Results of the Pathfinder Drilling Program Into a Major Growth Fault.: Part of the GBRN/DOE Dynamic Enhanced Recovery Project in Eugene Island 330 Field, Gulf of Mexico (CD-ROM). Lamont-Doherty Earth Observatory Press.

4. Hart, B.S., P.B. Flemings, and A. Deshpande. 1995. "Porosity and Pressure: Role of Compaction Disequilibrium in the Development of Geopressures in a Gulf Coast Basin." Geology. Vol. 23, No. 1, pp. 45-48.

5. Roberts, S.J., and N.A. Nunn. 1995. "Episodic Fluid Expulsion from Geopressured Sediments." Petroleum Geology. Vol.12, pp. 195-204.

Unreported publications and abstracts from previous quarters:

1. Whelan, J.K., L.B. Eglinton, and L.M. Cathles III. 1994. "Pressure Seals: Interactions with Organic Matter, Experimental Observations, and Relation to a "Hydrocarbon Plugging" Hypothesis for Pressure Seal Formation." In: *Basin Compartments and Seals.* P. Ortoleva & Z. Al-Shieb, eds, American Association of Petroleum Geologists Memoir 61, Chapter 7, pp 97-117.

2. Whelan, J.K., J. Seewald, L.B. Eglinton, and F.P. Miknis. 1994. "Time-temperature Histories of Kerogen and Mineral Ammonia from ODP Leg 139 (Middle Valley) Sediments." In: M.J. Mottl, E.E. Davis, A.T. Fisher, and j.F. Slack (Eds). *Proceedings of the Ocean Drilling Progam, Scientific Results, Vol.139*, pp 485-494.

3. Mao, S., L.B. Eglinton, J. Whelan, and L. Liu. 1994. "Thermal evolution of sediments from Leg 139, Middle Valley, Juan de Fuca Ridge: An Organic Petrological Study." In: M.J. Mottl, E.E. Davis, A.T. Fisher, and J.F. Slack (Eds). *Proceedings of the Ocean Drilling Progam, Scientific Results, Vol. 139,* pp 495-505.

4. Whiticar, M.J., E. Faber, J.K. Whelan, and B.R.R. Simoneit. 1994. "Thermogenic and Bacterial Hydrocarbon Gases (Free and Sorbed) in Middle Valley, Juan de Fuca Ridge, Leg 139."

In: M.J. Mottl, E.E. Davis, A.T. Fisher, and j.F. Slack (Eds), *Proceedings of the Ocean Drilling Progam, Scientific Results, Vol. 139*, pp 467-477.

5. Rowan, M.G. 1994. "Advantages and Limitations of Sections Restoration: Three-dimensional Geometry and Evolution of a Composite, Multi-level Salt Sheet, Gulf of Mexico: Modern Developments in Structural Interpretation, Validation and Modeling, Geological Society, London. February.

6. Rowan, M.G., P. Weimer, and P.B. Flemings. 1994. "Three-dimensional Geometry and Evolution of a Composite, Multi-level Salt System, Western Eugene Island, Offshore Louisiana: Gulf Coast Ass. Geol. Society Annual Meeting. Austin, Texas. October.

7. Rowan, M.G., McBride, B.C., Weimer, P., & Kligfield, R. 1993. "The Power of Section Restoration: Application to Deepwater salt structures from offshore Louisiana." Presented at the AAPG International Hedberg Research Conference on Salt Tectonics, Bath, England. September.

8. Luo, M., Wood, J.R. and L.M. Cathles. 1994. " Using Fabric Theory to Predice Thermal Conductivity in Reservoir Rocks Based on Rock Composition." Journal of Applied Physics. Vol. 32. pp 321-334.

Theses Completed:

1. Alexander, Laurel. 1995. Geologic Evolution and Controls on Fluid Flow of Eugene Island Block 300 Minibasin, Offshore Louisiana, Gulf of Mexico. Cornell Ph.D. Thesis. 206p.

7.3 U.S. Reserves Re-Evaluation:

This project is to perform a petroleum resource assessment for the Eugene Island area. The first step, to obtain data for the size and number of discovered hydrocarbon accumulations for the Eugene Island, Ship Shoal and South Marsh regions from Minerals Management Service, has been completed.

Using this data, the assessment methodology developed by C.C. Barton of the U. S. Geological Survey (*Barton and Scholz*, 1995; *Barton and Trussov*, in press) was applied. Additional work on the methodology and algorithm was completed for this project, to correctly complete assessments with the relatively limited data available for Ship Shoal, Eugene Island and South Marsh regions. Much of last July, August, September and October was spent further developing this methodology. The improvements to the algorithm benefited greatly by the recommendations of researchers at Woods Hole, Lamont, and Cornell. The methodology was applied to determine the size and number, and total volume of undiscovered conventionally recoverable oil and gas accumulations for Ship Shoals, Eugene Island and South Marsh regions. Table 1 presents some of the preliminary results for total volumes down to accumulation size of one (1.0) million barrels oil equivalent (mmBOE).

Table 1: Volumes of Undiscovered, Conventionally Recoverable Oil and Gas

	Gas		Oil	
	Percent Undiscovered	Volume Undiscovered (mmBOE)	Percent Undiscovere d	Volume Undiscovered (mmBOE)
Eugene Island	25%	971.	29%	612.
South Marsh	52%	2058.	28%	307.
Ship Shoal	57%	2776.	69%	3001.

Work remaining to be done is to finalize the above assessment calculations and complete preparation of a paper for publication. In addition, at the request of the Principal Investigator of the project, R. Anderson, with whom I met in April, I am attempting to obtain a breakdown of each region, into separate north (near shore) and south (off shore) divisions. These results would go beyond the work outlined in the subcontract. If the data can be obtained, and time permits, I will re-run each of the subdivided regions and include these results in the paper for publication and in the final report.

7.4 Technology Transfer:

1. Albert Boulanger and Wei He presented a poster at the Third SIAM Conference on Geosciences, San Antonio, February, 1995

entitled: "The Role of Pattern Recognition and High Resolution Inversion in Basin and MiniBasin Reservoir Characterization". In summary, the general problem of deducing geological structure and reservoir characteristics from a seismic signal is an ill-posed inverse problem. Solving the full 3-D inverse problem, for the basin scale in the time frame for production decisions is not feasible today. We described a methodology, based on the extraction of areas of interest within the 3-D volume by pattern recognition coupled with a high resolution inversion method, that allows for reservoir characterization questions to be answered.

2. The GBRN presented another large exhibition booth for this project at the Annual AAPG convention held in Houston, Texas the first week in March 1995. Although, this project and the CD-ROM was the main focus of the exhibit, the GBRN consortium solely carried the expenses of this year's exhibition booth.

3. Presentations and Posters presented at the Annual AAPG Convention, Houston, Texas in March 1995.

a. He, W., R.N. Anderson, X. Wang, and Y.-C. Teng. 1995. "Application of the 3-D FEM Seismic Modeling Technique in Reservoir Characterization and Fluid Monitoring." Presented at the AAPG Annual Convention. Houston, Texas. March.

b. Rowan, M.G., Villamil, T., Weimer, P., and P.B. Flemings. 1995. "Composite Origin of Allochthonous Salt, Offshore Louisiana." Presented at the AAPG Annual Convention. Houston, Texas. March.

c. Rowan, M.G. Villamil, T., Weimer, P., and P.B. Flemings. 1995. "Paleobathymetry and Paleotopography in the Gulf of Mexico: Comparison of Results from Cross-section Restoration and Biostratigraphic Analysis." Presented at the AAPG Annual Convention. Houston, Texas. March.

Reprints removed for separate cycling. [illegible]